DESIGN AND DEVELOPMENT OF DE-OXYGENATION SYSTEM AND TEMPERATURE CONTROL APPARATUS FOR NUCLEAR SPIN RELAXATION EXPERIMENTS

By

Walter Keith Oehlschlager

Bachelor of Science

Oklahoma State University

Stillwater, Oklahoma

1962

Submitted to the faculty of the Graduate School of
the Oklahoma State University
for partial fulfillment of the requirements
for the degree of
MASTER OF SCIENCE
May, 1965

DESIGN AND DEVELOPMENT OF DE-OXYGENATION SYSTEM AND TEMPERATURE CONTROL APPARATUS FOR NUCLEAR SPIN RELAXATION EXPERIMENTS

Thesis Approved:

V. L. Pollak

Thesis Adviser

H. E. Harrington

J. J. Boggs

Dean of the Graduate School

ACKNOWLEDGMENT

The author wishes to express his gratitude to Dr. V. L. Pollak for his guidance and assistance in the design and implementation of this study. Gratitude is also due the Army Research Office, Durham; Research Foundation, OSU, and the Petroleum Research Fund for equipment appropriations for this project. A note of thanks is due Richard Slater for his assistance in certain data-reduction techniques and opinions offered throughout this study.

TABLE OF CONTENTS

LIST OF TABLES

LIST OF FIGURES

CHAPTER I

DE-OXYGENATION OF LIQUID NMR SAMPLES

Introductory Statements

Since the presence of any dissolved paramagnetic oxygen tends to reduce the spin-lattice relaxation time, T_1, in liquids, it is essential that when studying organic liquids with long T_1's (i.e., $CHCl_3$, C_6H_6, etc.) the dissolved paramagnetic oxygen has been removed. This chapter outlines a procedure whereby a de-oxygenated liquid NMR sample may be obtained.

History

The efficiency of several simple processes of de-oxygenation was examined by Mears and Evans (1), and the residual oxygen content, measured as p.p.m., is shown in TABLE I. It can be seen that the most efficient process was the application of purified nitrogen through a scrubber, where the oxygen content was reduced to 0.0005 p.p.m. The oxygen was determined by the Risch modification of the Winkler method (2), by Potter and White (8).

Peers (3) devised a stationary platnimum micro-electrode and used it to determine residual oxygen by a polarographic technique (4). He measured the residual oxygen in solutions that had been de-aerated by the process of "freezing and thawing", a method then in use in his laboratories (5). In this process the solution was frozen with liquid nitrogen, the air was

removed by means of a vacuum diffusion pump and the solution was allowed to thaw. The cycle of operations was then repeated. Later the process was modified and the vacuum was applied to the solution for a short time immediately after it had thawed. Peers claimed that the efficiency of the original process could be increased by a factor of 5-10 if at the end of each cycle nitrogen was admitted to the apparatus; this ensured that the melting step of the next cycle was accompanied by the vigorous evolution of tiny gas bubbles from the surface of the melting ice; under such conditions the oxygen of the solution was reduced to 0.013 p.p.m., but that appeared to be the limit of estimation by this method.

The process of "flushing and boiling" was developed by Mills and Willis (6). The vessel containing the solution was evacuated with a rotary pump; consequently, the solution "boiled" owing to the evolution of dissolved gases; after a short time the pump was turned off and the vacuum destroyed by bubbling nitrogen through the solution; the cycle was repeated 4-5 times. The solution was not heated, but appreciable quantities of water vapor passed down the vacuum line and were absorbed in a large tube filled with calcium chloride.

The de-oxygenation technique to be outlined in the following chapter is an adaption of the Hersh technique (7), where the solution is scrubbed with purified oxygen-free nitrogen bubbles created by a fine dispersion frit. The nitrogen flow is adjusted to give conditions of such turbulence that maximum surface area contact with the nitrogen bubbles is attained.

TABLE I

METHOD OF DE-OXYGENATION	RESIDUAL OXYGEN, P.P.M.
Boiling for 6 min. and cooling	0.23[1]
Saturation with nitrogen, 2 min., followed by evacuation, 2 min., 4 cycles	0.20[1]
Saturation with CO_2, 2 min., followed by evacuation, 2 min., 4 cycles	0.17[1]
Evacuation, 15 min. followed by purging with nitrogen, 2 hr.	0.14[1]
Freezing and thawing, 3 cycles	0.13-0.07[3]
Freezing and thawing and flushing with nitrogen, 3 cycles	0.013[3]
Flushing and boiling	0.50-0.02[6]
Scrubbed with purified nitrogen, 1 hr.	0.0005[7]

Preparation of Oxygen-Free Nitrogen

The efficiency of the nitrogen bubbling technique is largely dependent on the degree to which the nitrogen has been de-oxygenated. The experimental scheme outlined here was devised by Arthur (9). It is a convenient method of removing oxygen from commercially available grades of nitrogen and other gases. The apparatus readily lends itself to our use because it is (a) efficient, convenient, and clean in operation, (b) self-indicating as to the condition of the charge, (c) ready to use even after standing for long periods without being used, (d) operates at room temperature and, especially important, since (e) it introduces no new components into the gas stream.

The scheme described here makes use of chromous sulfate formed in acid solution by reduction of chromic sulfate by amalgamated zinc. The reaction introduces small amounts of hydrogen into the gas, but fortunately

this hydrogen is harmless for our applications. On the other hand, the transparent blue color of the chromous solution contrasts so well with the dark green color of the chromic solution that the condition of the solution is readily apparent, while the formation of a precipitate indicates any need for more acid or for replacing both acid and chromic solution.

For the reactions involving these substances, the important equations are

$$Zn(Hg) + 2\,Cr^{+3} \longrightarrow Zn^{+2} + 2\,Cr^{+2} + Hg$$

$$4\,Cr^{+2} + O_2 + 4\,H_3O^{+} \longrightarrow 4\,Cr^{+3} + 6H_2O$$

while the principal side reactions are

$$2\,Cr^{+2} + 2\,H_3O^{+} \longrightarrow 2\,Cr^{+3} + 2\,H_2O + H_2$$

$$Zn + 2\,H_3O^{+} \longrightarrow Zn^{+2} + 2\,H_2O + H_2$$

Experimental

The de-oxygenation apparatus is shown in FIG. 1. The nitrogen passes, in order, through a safety trap, A, a scrubber, B, a second safety trap, A'; and a second scrubber, B'; then through a spray trap, E, and finally a drying trap, F. Since, when the gas flow is turned off solution usually moves back out of the scrubbers, traps A and A' are designed so that not only is this solution is forced back into the scrubbers. The scrubbers themselves are designed so that as the gas to be purified bubbles through the acid-chromous ion solution, the bubbles lift the solution and pump it over amalgamated zinc so the chromic ions formed are rapidly reduced again.

Vessels C and C' are bulbs into which the acid-chromium ion solutions from the scrubbers are forced by nitrogen pressure for storage when the

apparatus is put into stand-by condition. This conserves both the acid and the zinc - the only substances actually used up in the operation of the apparatus.

Part D, a pressure-relief value, was filled with mercury to a depth of 35 to 40 mm., a loose cotton plug to prevent spattering mercury being placed in the vertical tube K. The spray trap, E, was filled with indicating silica gel, with wads of glass wool at the bottom and top being used to keep drying agent in place. All standard joints were fastened using stopcock grease lubrication and wire clamps to keep joints from parting under gas pressure. All connective tubing was 3/16-inch I. D. Tygon tubing, and stopcocks G, H, and J were 4 mm. bore of the type apparent from FIG. 1.

Zinc rods ¼ inch in diameter and about 6 inches long and about ten in number were placed carefully in B and B'. A solution about 0.1 N with mecuric nitrate and 1 N with nitric acid was poured into B and B' to completely cover the zinc rods and allowed to stand for 60 minutes or until the rods were completely covered with mercury. When amalgamation was complete, the spent reagent was drained off and the rods were washed with distilled water. Finally, enough of a solution of 0.1 with chromic ion (chromic sulfate) and 3 N with sulfuric acid was added to B and B' to barely cover the upper end of the central tube; 50 ml. more added and drained into C and C' (using same N_2-pressure) to be used as volume replacement for exaporation. Then H was closed and stopcock G was turned to allow nitrogen to flow slowly through B and B'. According to Arthur[1], top efficiency is reached when the color of the solution changes from the green color of the chromic state to the blue of the chromous state. This was not observed experimentally, however the blue chromous color could have

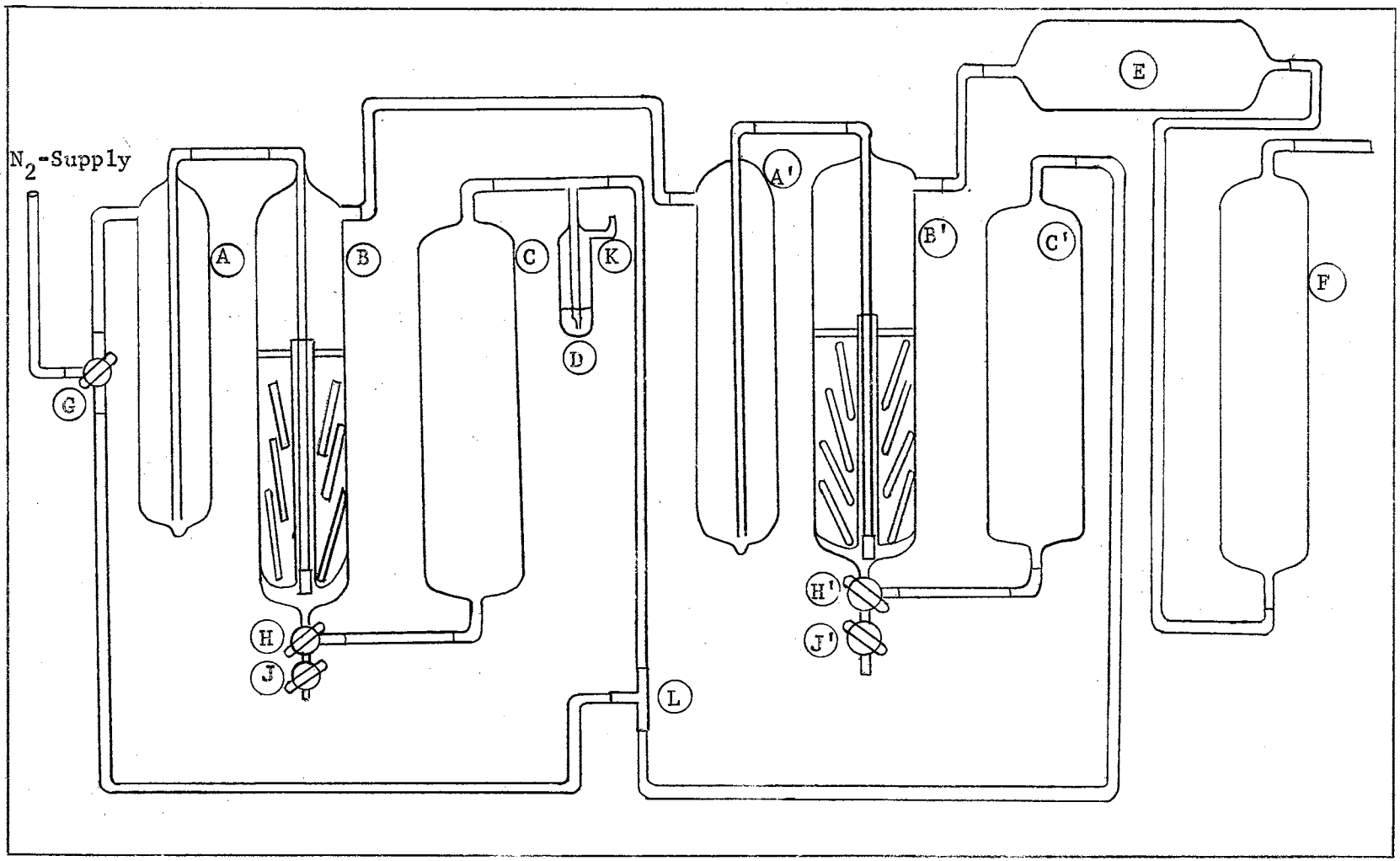

Figure 1. Preparation of Oxygen-Free Nitrogen

easily been masked by the dark green chromic solution.[1] When the apparatus was not in use the solution was transferred from B and B' to storage bulbs C and C', respectively. Transfer from B was accomplished by opening stopcock H to connect B to C and same nitrogen pressure used to force the solution from B into C. The gas in vessel C is expelled through the pressure release valve at K. Finally, H was closed to prevent return of the solution to B. By similar action, the solution is transferred from returning to B'. During such storage, any blue chromous ion will disappear by reaction with the acid and water, the pressure developed by the hydrogen so formed being vented from both C and C' through the pressure-relief valve D.

When the solution is stored in C and C', all reaction ceases once the solutions still wetting the amalgam and the chromous ions in the solutions in C and C' are used up. Consequently, even after months of standing the apparatus can be reactivated within moments.

To do this, G was turned so a slow stream of nitrogen flowed into L, and the following procedure carefully used. H' was opened so C' was connected to B', and K and the outlet from F were closed. Nitrogen pressure forced solution from C' to B'. The gas in vessels B' and B is allowed to escape by temporarily opening the pressure relief valve at K. When enough solution was in B, H' was closed and H opened to connect C to B, forcing solution from C into B. Finally, H was closed and G turned so that nitrogen flowed through A.

PREPARATION OF DE-OXYGENATED NMR SAMPLES: $CHCl_3$

---

[1] Private Communication, Dr. Arthur, OSU Chemistry Department

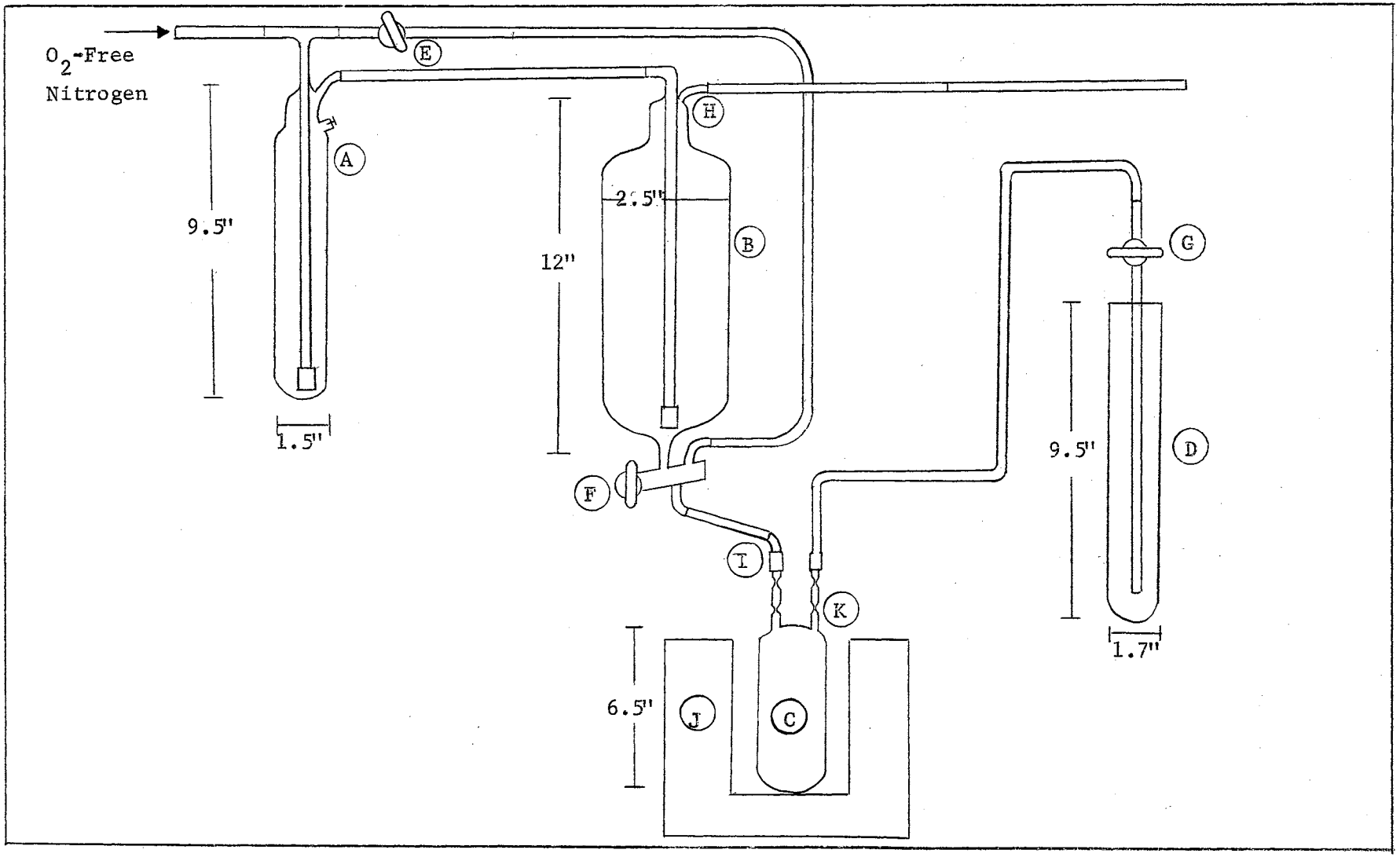

Figure 2. De-Oxygenation Apparatus

The apparatus concerned is shown in FIG. 2, consisting of four main parts, the saturator, A; the de-oxygenation scrubber, B; the sample bottle, C, and the bubbler, D. All connective tubing that comes in contact with the liquid vapors is made of teflon 3/16" I.D. Teflon was used because $CHCl_3$ readily dissolved the rubber and tygon tubing which was installed originally. A teflon stopcock was employed on B, along with a 24/40 teflon sleeve for the ground glass joint. A 2 mm. capillary tube was connected to the outlet H between the de-oxygenation chamber and the atmosphere to minimize the effect of back diffusion. Stopcocks G and F are 4 mm. ground glass type, lubricated with silicone grease.

The liquid to be de-oxgenated and permanently sealed is poured into A and B, the liquid level in A should be approximately 1 inch from the top and the level in B should be 2 inches from the top, and D is filled with water. The liquid levels in A and B are approximate and are meant to assure that the bubbling action of the liquid in the vessels does not cause unnecessary mixing. The saturator, A, prevents the dry-N_2 from evaporating the sample liquid in B by first saturating the nitrogen by bubbling through a fine dispersion frit which is placed at the end of an 8 inch glass tube in A. A fine dispersion frit is also employed in the de-oxygenation bottle, B, to provide maximum surface area contact of the liquid with the nitrogen bubbles. The teflon tubing used throughout the system was attached to the glass by expanding the ends with a propane torch, fitting them over the glass tubing, and allowing them to cool, thus providing as good a vacuum tight seal as possible. At I., one-inch tygon sleeves are used to connect the sample bottle to the de-oxygenation apparatus. Here, the tygon comes in contact with the liquid when it is transferred into C. Contact lasts for approximately 5-minutes, during transfer.

With liquid in the vessels A and B, F closed to B, G and E open, oxygen-free nitrogen, obtained from the apparatus shown in FIG. 1, is allowed to flow into the system and proceeds as follows. The nitrogen flows along two different paths designed to (1) saturate and de-oxygenate and (2) continually flush the sample bottle, C, with nitrogen. The path along (1) proceeds through the frit in A, then to B where the actual de-oxygenation takes place, and finally through outlet H, the glass capillary tubing and out to the atmosphere via latex tubing. Since $CHCl_3$ vapors are harmful, the latex tubing leads to the outside atmosphere. The second path, (2), proceeds through E, through the three-way teflon stopcock F which is closed to B but open to I and C. This allows dry-N_2 to continually flush the sample bottle during the de-oxygenation process. The rate of flushing being regulated by the stopcock E, and observed by the rate at which nitrogen bubbles appear in D.

The nitrogen is allowed to bubble through the system for as long as required to de-oxygenate. This may be anywhere from 3 hrs. (± 1 hr.) for benzene, to 24 hrs. (± 2 hrs.) for chloroform. When ready to terminate the de-oxygenation process and permanently seal off the sample, the following procedure is used. Reduce nitrogen pressure slightly. Open F to B and C, thus stopping the flushing action through C and allowing the de-oxygenated liquid to flow into C, which contains a nitrogen atmosphere. As the liquid is transferred to C, nitrogen will be forced from the bottle and bubble through D. This eliminates all possibility of back-diffusion of air while transferring the sample liquid. A slight nitrogen pressure is maintained in A and B, actually forcing the liquid into C. The liquid is allowed to fill C except for approximately 50 cc. of free volume at the top. This is to compensate for volume expansion of the liquid at higher

temperatures.*

When the liquid level has reached the desired height in C, F is closed, stopping the flow of liquid. F is turned so that again dry-N_2 is allowed to flow through I and bubble up through D. This allows the nitrogen to dry the tubing through which the liquid has just past. It is particularly important that when the liquid is $CHCl_3$ (or other volatile liquid), the capillary constrictions at I be completely dry, since sealing requires application of gas flame at these points. This drying procedure should not take more than 10 minutes. To isolate liquid in C, close F and G.

The styrafoam container, J, is then filled with salt and ice, packing the area around the sample bottle C. The temperature of the ice-salt mixture will reach approximately $-10^{o}C$, in approximately 10 minutes. As the temperature of the sample drops from ambient, a partial vacuum is formed in the free volume above the liquid. After about 30 minutes of cooling the sample, a permanent seal is performed by applying a gas flame jet to the capillary constriction attached to the sample bottle, at K. The vacuum created within C aids in the sealing process, and prevents a build up of positive pressure when the flame jet is applied. Once sealing is complete, the container J is emptied of ice and salt and the permanently sealed, de-oxygenated sample is removed.

The technique for obtaining non-permament samples is slightly different. A sample bottle is used which has two stopcocks attached at K; teflon stopcocks being utilized in the case of $CHCl_3$ or other organic solvent in A and B. Once de-oxygenation has been terminated, the liquid is transferred as before by turning F to allow nitrogen pressure to force the

---

*See Suggestion for Samples to be Studied at Elevated Temperatures.

liquid into C. Once transfer is completed, F and G are closed. Completion of the sealing off procedure merely requires the stopcocks at K to be closed, and tightened, if possible.

Experimental Verification of De-Oxygenation Technique

Benzene was chosen to study the actual efficiency of the de-oxygenation technique. A 400 ml. sample of de-oxygenated benzene was prepared; the minimum time required for de-oxygenation being approximately three hours. The spin-lattice relaxation time, T_1, was measured utilizing the earth's field free precession apparatus available (13). The measured value of T_1 = 18 seconds in a field of 500 gauss agrees with the experimental results of Paules and Cutler (14) and also with those of Nederbragt and Reilly (15), where the freeze-pump-thaw technique was used to de-oxygenate.

The value of T_1 in the earth's field (0.54 gauss) was measured to be in 18 sec, implying either that Paules and Cutler's value of T_2 = 11 sec. at 250 gauss is wrong or that the field dependence for T_1 occurs at fields lower than the earth's field.

Suggestion for Samples to be Studied at Elevated Temperatures

To avoid pressure build up when sample temperature is raised above that at which de-oxygenation was carried out, the salt-ice bath can be replaced by a dry ice or liquid nitrogen bath, so that the liquid sample (c) freezes. (We assume the sample liquid is one that does not expand on freezing.) The space above the sample can then be evacuated by connecting a vacuum pump at D, and opening G. After seal-off, the sample can be raised to the boiling point before any positive pressure develops.

CHAPTER II

TEMPERATURE CONTROL

The Apparatus

A schematic of the temperature control apparatus is shown in FIG. 3 (a) and (b). The heart of the system is the Haake Model NBS Constant Temperature Circulator. This unit thermostatically controls the temperature of the circulating liquid in the bath reservoir to within ± 0.04°C of the desired temperature within the range from -60°C to +150°C. The Haake Model NBS circulator consists of the following main components: (A) Housing with inner copper reservoir, the insulation between the vessels being glass wool, (B) Two heating elements (700w and 1000w) which can be operated singly or together, (C) A control unit consisting of a Contact Thermometer in combination with a gas filled vertical mercury relay to regulate the bath temperature, and (D) A rotary pump, with flexible coupling, twin outflow and return nozzles for external pressure circulation of the tempering liquid. The circulator utilizes two pumping actions, a pressure action and a suction action. The combined circulating capacity utilizing both the pressure and suction nozzles in 7 gal/min. With suction only, the maximum flow rate is 2½ gal/min.

The physical layout of the NMR apparatus is such that the electronic equipment and circulator are housed in a quonset building, with the coils (into which the sample is to be inserted) mounted rigidly on a wooden

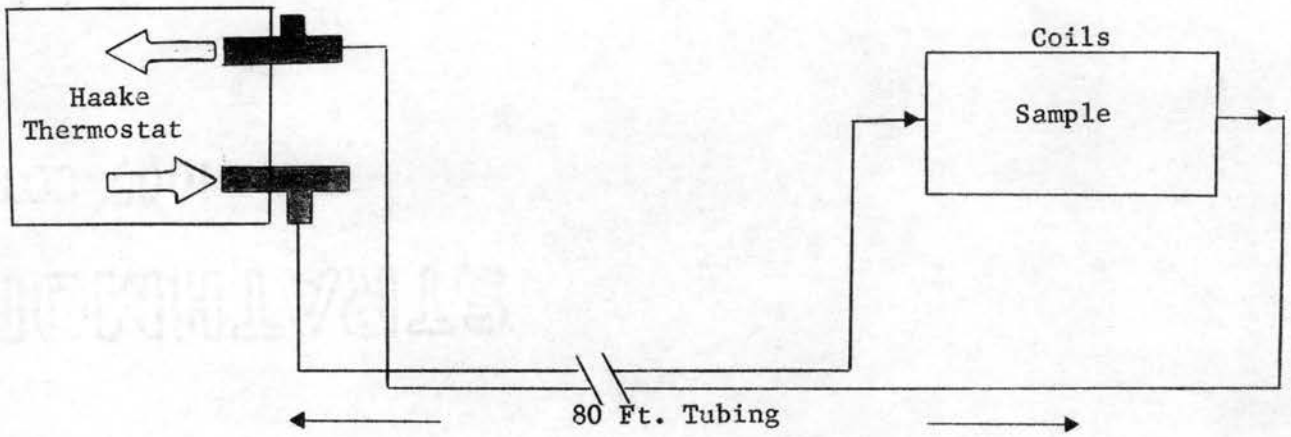

(a) High Temperature Range

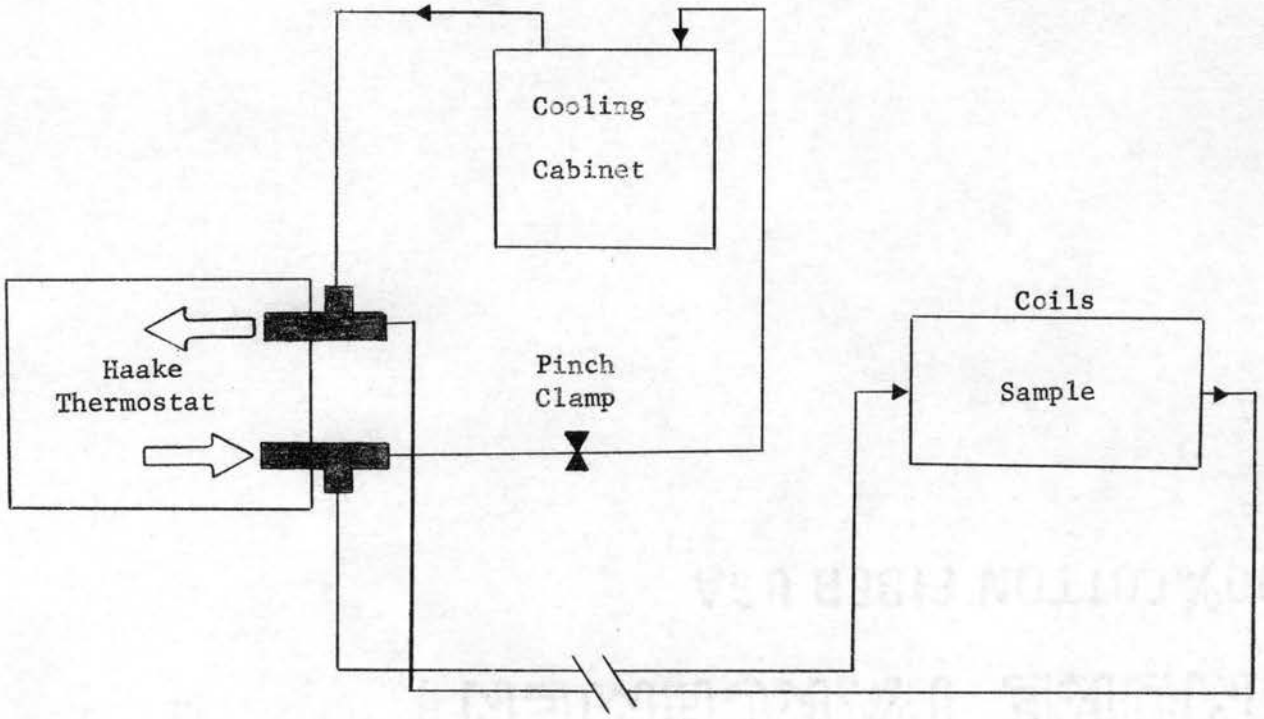

(b) Low-Temperature Range

Figure 3. Temperature Control Schematic

platform 75 feet from the quonset. This is to isolate the coils from any ferromagnetic materials which might contribute to the nonuniformity of the earth's field. Thus, a 90 foot long cable was used to connect the coils at the platform with the electronic equipment inside the quonset. The tempering liquid was pumped from the quonset to the coil site.

As shown in FIG. 3, copper tubing (I. D. = ½ inch, O. D. = 5/8 inch) was used to transport the circulating liquid to and from the coil site. Approximately 160 feet of tubing was used with brass flared-coupling joints utilized to connect the tubing, which was supplied in 60 foot sections. The copper tubing was insulated with a ½ inch layer of Armstrong Rubaflex insulation. Armstrong adhesive glue was used to connect the 6 ft. lengths of the insulation, providing a leak proof seal. The joints were then wrapped with several turns of aluminum tape to give a better seal. Insulated perbunan rubber tubing was used to connect the sample enclosure at the coils to the copper tubing, and also between the copper tubing at the quonset and the pump and suction nozzles on the circulator. Approximately 80 ft. of aluminum pipe (I. D. = 4.00 inch O. D. = 4.05 inches) was used to encase the electrical cable and insulated copper tubing, providing for additional electrical shielding and serving to isolate the cable and tubing from the elements. The aluminum pipe was connected at 20-ft. sections by non-permanent aluminum sleeve joints, allowing the cable and tubing to be accessable for repair and/or removal. The aluminum sleeve joints fit snuggly over the pipe and calking compound was used to seal the joints, finally wrapping the entire joint with one-inch aluminum tape. The pipe was buried approximately 1½ feet below ground level in a 6-inch bed of sand to isolate the pipe from the acidic soil, extending above ground only at the coil site and at the outside entrance into the

quonset wall.

The design of the glass sample enclosure is shown in FIG. 4, where the sample, (A), is mounted centrally in the coils (G), positioned inside the glass container (D). Glass indentations at (E) and (F) position and hold the sample bottle in the center of fluid flow, allowing no horizontal movement while circulating. A flared glass joint was used at (B), with a plastic clamp used to fasten the joint tightly with nylon screws. Silicone lubricant was used at (B) to provide a vacuum seal under pressure. The temperature of the circulating liquid was monitored by a thermometer with a 10/30 ground glass joint mounted and fastened at (C).

Operation Procedure With Haake Circulator

For closed circuit tempering of the sample, the tubing is connected from the outlet nozzle to the sample enclosure at H. The return hose is connected from J to the return nozzle with suction. The flow rate depends on the flow resistance, length of connections, dimensions of sample jacket, viscosity, elevation, etc.

The bath and external circuit was filled so that the liquid height in the reservoir was approximately two inches from the top. If the liquid level is too high, pumping efficiency decreases; if too low, heater and pump may burn out.

For the temperature range from -60°C to +100°C, two contact thermometers were employed within the thermostat; one from -60°C to +30°C and one from 0°C to +100°C. The desired control temperature was set on the vacuum sealed contact thermomenter in the manner described in the Haake Manual.

After the bath had come "up" or "down" to the desired temperature, the "actual" bath temperature was read on a control thermomenter inserted

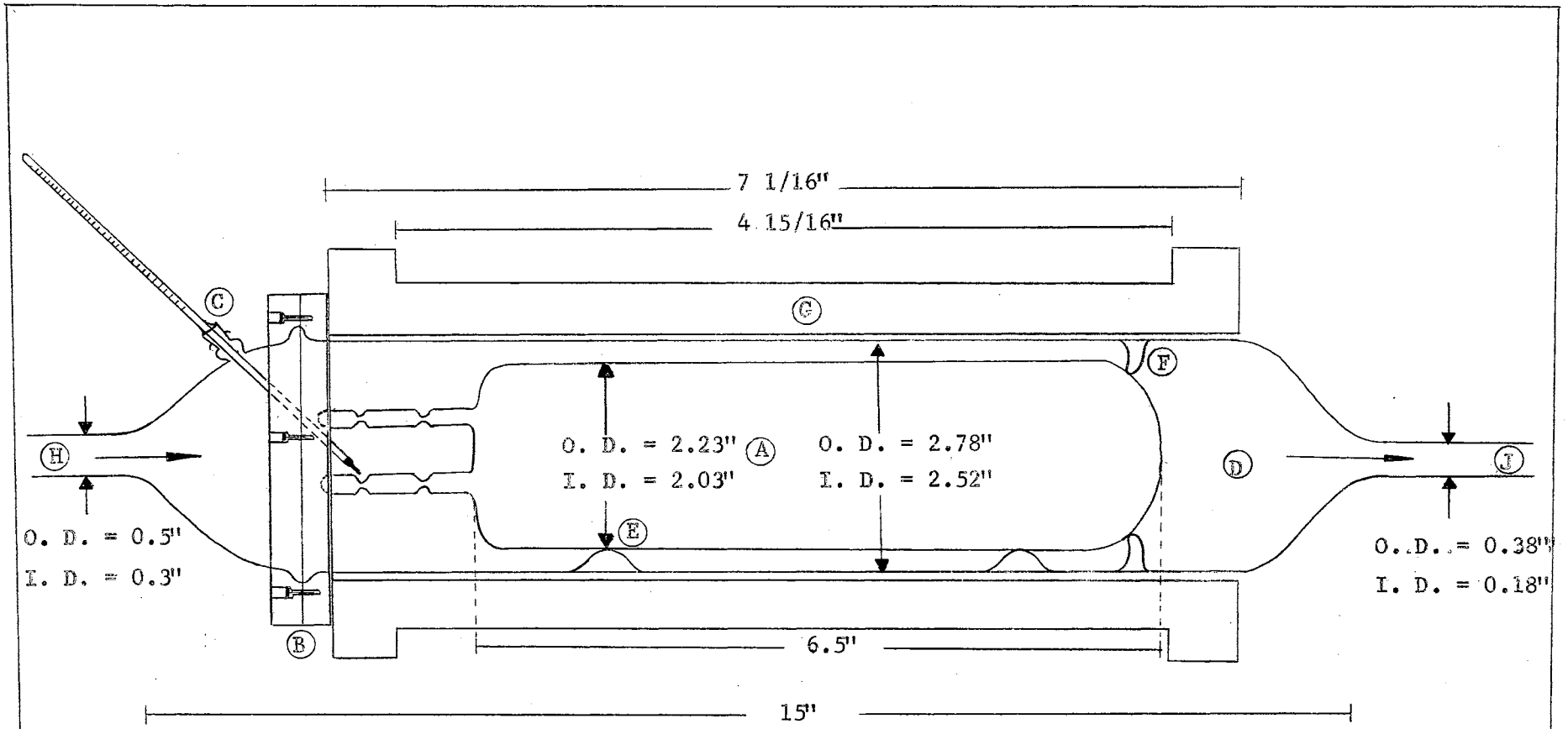

Figure 4. Sample and Enclosure at Coil Site

in the bath liquid. The actual temperature may differ from the setting of the contact thermometer by approximately 0.5 degrees.

The heating control is by two heaters, either operated individually or combined. Normally, the 1000 watt heater is used only for rapid heating up since the 700 watt heater provides more stable control once the desired temperature has been reached. The heaters are operated only when the pump is in operation, and thus preheating of viscous liquids can only be accomplished by placing an extra immersion heater in the bath.

High Temperature Operation

The liquid circulated in the temperature range from $+10^{\circ}C$ to $+100^{\circ}C$ was distilled water. The water was made slightly basic (ph$\sim$8.00) by the addition of ammomium hydroxide. A paramagnetic salt, $NiSO_4$, was used to reduce the T_2 of the water to below 40ms. Nickelous sulfate was used because of its low electronegativity and great solubility in dilute NH_4OH solution. Also, the bath reservoir is constructed of a nickel-steel alloy and the possibility of a displacement reaction with $NiSO_4$ in solution was rendered harmless. A systematic study is currently under way in which various suitable paramagnetic salts will be investigated to determine the extent to which the T_2 of the circulating water may be reduced.

The control accuracy was maintained by the cycling of the 700 watt heater, the 1000 watt heater utilized only to reach the desired temperature. The entire thermostat was insulated with a one-inch layer of foam rubber, except for the control relay box and pump motor housing. Ventilation is obtained by air sucked in through the openings in the bottom of the relay box and these should not be obstructed in high temperature operation.

With the pumping circuit shown in FIG. 3 (a), control accuracy at the coil site was maintained to within $1^{o}C$ of the desired temperature within the range from $10^{o}C$ to $85^{o}C$. The control depending, of course, upon ambient conditions and time of day; i.e., day or night.

Since the thermometer (c) in FIG. 4 monitors only the temperature of the circulating liquid and not the actual sample temperature, a sample enclosure was designed to investigate the internal tempering of the sample. The apparatus is shown in FIG. 5, where a sample bottle, (A), identical in shape to the one in FIG. 4, is permanently sealed inside the glass container by flared connections at (B). A thermometer, (D), with a 10/30 ground glass joint is mounted in the socket at (C) which allows the temperature of the liquid in (A) to be measured, while also monitoring the temperature of the circulating liquid by a thermometer inserted at (E).

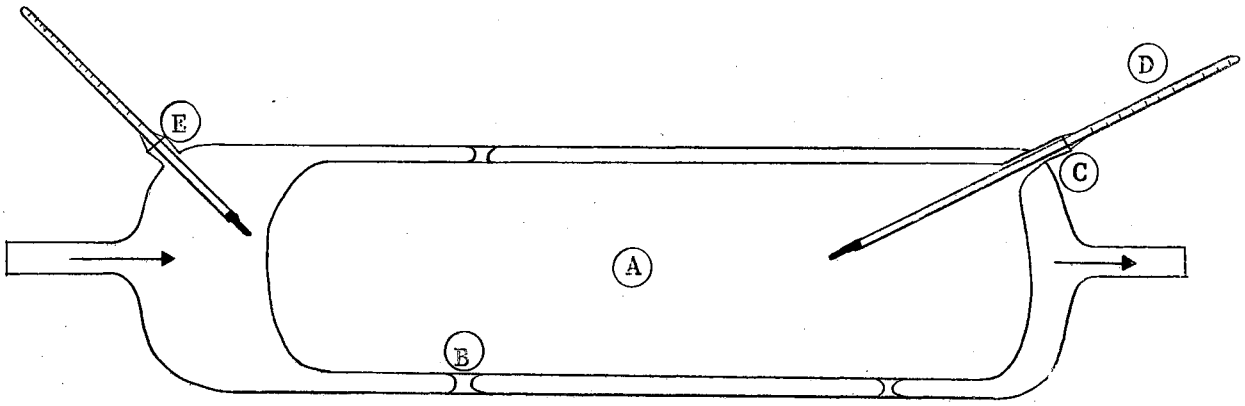

FIGURE 5. Sample Enclosure

The correlation between the sample temperature and the surrounding liquid temperature was found to be within $\pm$ $0.05^{o}C$ for the range from $+25^{o}C$ to $75^{o}C$. The ambient temperature was $23^{o}C$. For water it was observed that it required from 5 to 10 minutes for the sample temperature

to reach the control liquid temperature. Hence, when T_1 measurements were begun, 30-minutes was allowed for the sample to reach the control temperature.

Low Temperature Operation

The circulating liquid used in the temperature range from -40°C to +10°C was methyl alcohol; freezing point = -98.3°C. The methanol T_2 was reduced to less than 20 ms. by the addition of $MnCl_2$, which readily dissolves in methanol.

An integral part of the low temperature operation is the cooling cabinet, shown in FIG. 6. The cabinet is constructed of three heavy-walled plastic containers, insulated between each container with a one-inch layer of foam rubber. Copper cooling coils (O. D. = 3/8 in.) wound around a 6-inch diameter, 20 turns, separated by approximately ½-inch space, are used in the cooling cabinet as shown in FIG. 6. A loose fitting plastic cover, insulated with a 3-inch layer of foam rubber fits snuggly over the cabinet, with a small opening at the top to prevent CO_2 pressure built up when using dry-ice and acetone around the coils.

As shown in FIG. 3 (b), the same liquid is circulated through the cooling coils and the external circuit. Referring to FIG. 3 (b), the flow rate, and thus the cooling rate, is regulated by a pinch clamp on the hose connecting the coils to the thermostat. Ideally, it should create a ratio of heating: cooling time which is 1:5 (Refer to Manual 104). Experimentally the ratio varied from 1:4 to 1:10, depending upon the control temperature desired. Down to ambient and temperatures around 10°C, ice and salt were used in the cooling cabinet, while a dry-ice and acetone

mixture was used to reduce the bath temperature from +10°C to -30°C. Approximately 30 lb/hr. dry-ice was required to reach a constant control temperature of -30°C (± 0.5°C), the ambient temperature being 23°C. Control accuracy was maintained to within 0.5°C of desired temperature within the range from -30°C to +10°C. The regulation depending, of course, upon ambient conditions, time of day, etc.

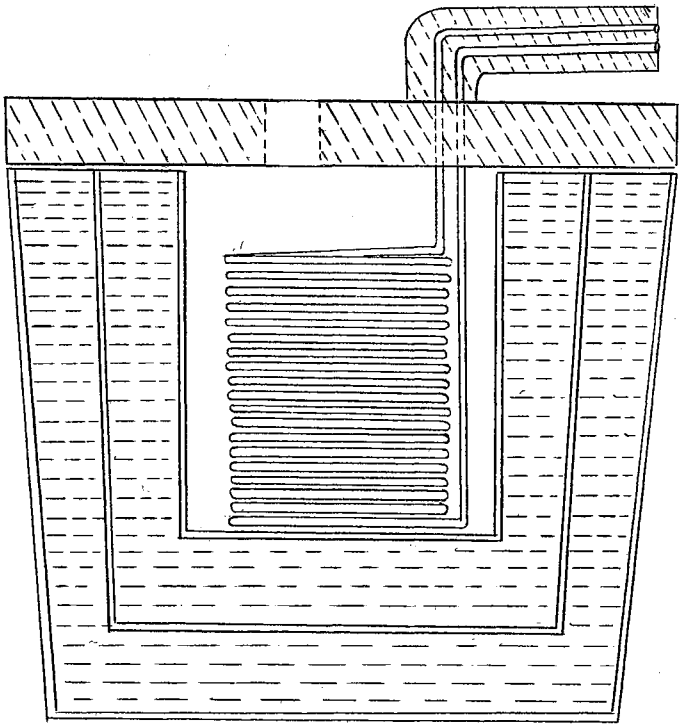

FIGURE 6. Cooling Cabinet

When operating at low temperatures ($T < 0^{\circ}C$) for prolonged periods, the motor and electrical system were protected against water condensation by supressing the flow of cold air room the motor fan. This was accomplished by covering the openings on top of the motor housing with a foam rubber cap. Also, the air entry slot underneath the relax box was covered with an adhesive tape.

Since the two circulating liquids, water and methanol, are soluble in each other; thorough cleaning of the circuit and thermostat is not

necessary when changing fluids. A dry-nitrogen tank was installed near the thermostat so that nitrogen gas under pressure could be used to flush the liquid from the external circuit and allow an easy, clean, and efficient method for changing liquids.

Future Improvements

Because of the large demand for dry-ice with the present cooling system, a mechanical refrigeration system would be more efficient and economical in the future. The possibility of utilizing such a mechanical system is being investigated at the present time.

Although the use of thermometers has been sufficiently accurate to measure the temperature, it would be more convenient to employ a thermistor at the coil site which could be monitored inside the quonset.

Improvements could be made on the insulation around the sample, possibly housing the tubing in an aluminum duct which would lead directly up to and away from the coils.

Design Factors

Environmental factors considered in the design of the temperature control system included (a) the geometry of the sample coil, (b) use of non-magnetic materials at the coil site, (c) fluctuations in ambient temperature.

It was found that factors (a) and (b) imposed no serious limitations on the design. The 3 inch I. D. of the coils allowed a 400 ml. sample bottle to be centrally positioned inside, with approximately 0.3 inch space between bottle and coils to allow a suitable chosen fluid to flow

completely around the vessel to provide thermal control of the sample. Control accuracy was, of course, dependent upon (c), however temperature variation to within $\pm$ 0.5°C was easily obtainable in most cases. However, when changes in ambient temperature occurred rapidly (i.e., sunset, sunrise) the temperature variation was observed to be as much as $\pm$ 1°C.

Some of the experimental factors considered in the design of the temperature control system included: (a) the desired temperature range, (b) time of duration required at desired temperature, (c) control accuracy desired; and (d) the presence of an n.m.r. signal from the liquid to be circulated around sample.

The temperature control system designed is capable of reaching temperature within the range from -30°C to +100°C, and maintaining control fluctuation to within $\pm$ 1.°C for periods up to three or four hours. This meets the experimental requirements imposed by factors (a), (b), and (c). Doping the circulating liquid with a suitable paramagnetic salt, thus reducing the T_2 of the signal to below 50 ms, was found to be an adequate solution to (d). Since the shortest T_2 measured for de-oxygenated $CHCl_3$ was greater than 1.5 sec. (in earth's field, 0.54g.) the transient signal from the doped circulating liquid did not hinder T_1 measurements on $CHCl_3$.

The probelm of a-c noise was a dubious one, but it was found that gounding the copper tubing to the aluminum pipe incasing the tubing reduced the noise level by a factor of two. Further reduction in the a-c noise level resulted when a common ground was used for the Haake circulator and the electronic equipment employed.

A theoretical calculation was made of the expected heat losses

throughout the temperature control system, both at the coil site and along the insulated tubing. The principal causes of steady-state heat losses considered were by conduction and radiation. Throughout the calculations, the specified flow rate of 2½ gal/min[2] was used, with water being used for high temperature calculations and methanol for the low temperature case.

The derivation of the conduction heat flow equation for concentric cylinders proceeds as follows. The quantity of heat transmitted through a cross-sectional area of A cm^2 in one second is given by Fourier's law as,

$$H = k\,A\,\frac{dt}{dL} \tag{1}$$

where k = thermal conductivity (cal/sec-cm^{o}-C); $\frac{dt}{dL}$ = temperature gradient across dL.

Consider a composite tube wall, with inner diameter Di and outer diameter Do, and length L. Then integration of Eq(1) gives a radial heat current

$$H = \frac{2\pi kL}{\ln\, Do/Di}\ (ti - te)\ \frac{cal}{sec} \tag{2}$$

For the extreme high temperature case where water at ti = 100°C is circulated around the sample, the steady state heat loss via conduction from sample enclosure (FIG. 4) was calculated, where the insulation between the enclosure (ti = 100°C) and coils (te = 25°C) was felt (k = 0.000087 cal/sec-cm-°C). Do = 7.62 cm, Di = 7.06 cm, and the length of the enclosure, L = 38 cm. Using eq. (2), the expected conduction heat loss,

---

[2]Operating Manual 104, Series N Haake Circulators.

H, over the length of the enclosure was 84.6 watt. The conduction heat gain in the extreme low temperature case was calculated where ti = $-60^{o}C$, te = $+ 25^{o}C$, and gave a value of H = 96.6 watt.

In calculating the conduction heat loss in the insulated copper tubing (length L = 160 ft.) the value of k for the Rubaflex insulation was not available, and the value of k = 0.00045 cal/sec-cm-^{o}C for rubber was used in eq. (2). Assuming ½-inch insulation around the tubing, where ti = $100^{o}C$, te = $+ 25^{o}C$, yields an expected heat loss of H = 4360 watt over the total length of the tubing.

Since the heat released, H, is equal to the heat loss of liquid flowing at rate F cm^3/sec, then

$$H = F\ cp\ \Delta T \rho \tag{3}$$

where F = 2.5 gal/min (158 cm^3/sec), cp = specific heat of circulating liquid (cal/gm^{o}C). ΔT = temperature change of liquid (^{o}C), and ρ = density of liquid (gm/cc). For the case of water at Ti = $100^{o}C$ circulating through the tubing, H = 4360 watt, and eq. (3) yields $\Delta T = 6.5^{o}C$. Thus, the expected temperature drop of water from the thermostat to the coil site is approximately three degrees.

The radiation heat loss was also calculated for the sample enclosure. The rate of absorption or radiation of radient energy per unit area by a body at temperature T is given by Stefan's law as

$$R = \sigma e T^4,$$

where e is the emissitivity of the material, T is the absolute temperature (^{o}K), and σ has the value of 5.67×10^{-8} Watt/M^2 $(^{o}K)^4$. Thus, for a body at a temperature T_1 surrounded by a material at a temperature T_2, the net

rate of loss (or gain) or energy by radiation is

$$H = A e \sigma (T_1^4 - T_2^4) \quad (4)$$

where H is the heat loss (or gain) in watts and A is the surface area of the body.

Calculating the heat loss via radiation from the sample enclosure in the coils, where $T_1 = -60^{\circ}C$, $T_2 = 40^{\circ}C$, e = 1 (assume black-body radiation), A = 842 cm^2, yields H = 36.3 watt. For the extreme high temperature case, where $T_1 = 100^{\circ}C$, $T_2 = 40^{\circ}C$, eq. (4) gives H = 49.2 watt.

Calculating the radiation heat loss from the pipe (L = 160') where $T_1 = -60^{\circ}C$, $T_2 = 40^{\circ}C$, e (Cu) = 0.3, A = 24, 300cm^2, yields H = 314 watt. And, also for the high temperature case, where $T_1 = 100^{\circ}C$, $T_2 = 40^{\circ}C$, eq. (4) gives H = 432 watt.

Combining the calculated heat losses by conduction and radiation for the high temperature case, yields a total H = 4926 watt, and calculating the expected change in temperature from thermostat to the coils yields $\Delta T = 3.7^{\circ}C$. Experimentally it was observed that the temperature drop from the circulator to the coils was approximately $1^{\circ}C$ for the extreme high temperature case, ($T_1 = 50^{\circ}C$, $T_2 = 25^{\circ}C$) and also $1^{\circ}C$ change for the extreme low temperature case, ($T_1 = -30^{\circ}C$, $T_2 = 23^{\circ}C$). This differs from the theoretical prediction by a factor of 3, however, the conduction heat loss along the tubing was less than calculated since the insulation used was porous rubber rather than solid rubber as used in the calculations. Also the temperature gradient observed experimentally was always less than the value used in the calculations. The radiation and conduction heat losses at the thermostat itself were not calculated since they were small compared with losses at the coil site and along the tubing.

CHAPTER III

TEMPERATURE AND FIELD DEPENDENCE OF T_1 IN $CHCl_3$

Theoretical Spin-Lattice Relaxation Time

The spin-lattice relaxation time, T_1, in liquids may be written as

$$\frac{1}{T_1} = \frac{1}{T_{1(rot)}} + \frac{1}{T_{1(trans)}} \tag{7}$$

where the contributions arise from the rotational and translational movements, respectively, of the molecules.

Theoretical expressions for these contributions have been derived (16, 17) and are given below:

$$\frac{1}{T_{1(rot)}} = 2\pi \frac{\gamma_p^2 \gamma_{cl}^2 \hbar^2 a^3 \eta}{b^6 kT} \cdot n \tag{8}$$

$$\frac{1}{T_{1(trans)}} = \frac{6\pi^2}{5} \gamma_p^4 \hbar^2 \frac{N\eta}{kT} \tag{9}$$

For the case of the dipole-dipole interaction in $CHCl_3$, γ_p = 4.26 kc/g, γ_{cl} = 0.42 kc/g, N = number of molecules per unit volume, a = molecular radius of $CHCl_3$, η = viscosity, b = intermolecular proton-chlorine distance, $k = 1.38 \cdot 10^{-16}$ erg $(^oK)^{-1}$, T = temperature (^oK), and n = number of equivalent nuclei of spin S.

Assuming hexagonal close-packing of hard spheres, the molecular radius, a, was calculated for $CHCl_3$ to be 3.26 Å . The intermolecular proton-chlorine distance, b, was calculated from molecular structure data (18) to be

2.34 Å. The viscosity η = 0.005 poise at T = 39°C and the value of γ_{Cl} = 0.42 kc/g was used since this value corresponds to the 75% abundant isotope of chlorine.

From eq. (8) the rotational contribution was calculated to be T_1 = 1140 sec, and the calculated value of the translational contribution from eq. (9) was T_1 = 140 sec. Substituting these values into eq. (7) yields a spin-lattice relaxation time T_1 = 128 sec at 39°C for $CHCl_3$ in high field. Experimentally, the spin-lattice relaxation time in de-oxygenated $CHCl_3$ at 40°C in 500 gauss was found to be T_1 = 100 sec (± 10 sec), in reasonable agreement with the theoretical prediction.

A possible source for this discrepancy could be in the calculation of "a", the molecular radius. Since the $CHCl_3$ molecule is a symmetric top molecule, assuming hexagonal close-packing may be an invalid approximation. Also the presence of dissolved paramagnetic oxygen (remaining after de-oxygenation procedure is terminated) could lower T_1.

Field Dependence of T_1 in $CHCl_3$

The chlorine magnetic relaxation times for $CHCl_3$ may be calculated by quadrapole interactions since the chlorine nucleus has a finite quadrapole moment and is situated in a molecular environment of non-cubic symmetry. The theoretical expressions for the proton spin-lattice relaxation time, T_1, and the spin-spin relaxation time, T_2, have been derived (16) and are given by

$$\frac{1}{T_1} = DD + n \cdot \frac{2}{3} J^2 S(S+1) \left[\frac{\tau}{1 + (\omega_1 - \omega_s)^2 \tau^2} \right] \tag{10}$$

$$(11) \qquad \frac{1}{T_1} = DD + n \cdot \frac{J^2}{3} S(S+1) \left[\frac{\tau}{1 + (\omega_1 - \omega_s)^2 \tau^2} + \tau \right]$$

where the first term DD represents the contribution to $1/T_1$ and $1/T_2$ from the dipolar coupling with other spins. The spin S of the chlorine nucleus is equal to 3/2. The contribution of the first term is the same for T_1 and T_2 and independent of the nuclear frequency because of the very short correlation time of the dipolar coupling. The second term in eq. (10) represents the effects of the scalar coupling term $J\hbar\vec{I}\cdot\vec{S}$.

In general, for two nuclear spins I and S, the indirect scalar coupling $J\hbar\vec{I}\cdot\vec{S}$ is usually much smaller than their ordinary dipolar coupling. However, this does not mean that the corresponding relaxation mechanism is negligible, since the correlation time τ may be much longer than the rotational correlation time, and this may increase considerably the relative relaxing effectiveness of the scalar coupling as compared to that of the dipolar coupling. As a consequence of this fact, from eq. (10) and (11) since $(\omega_1 - \omega_s)\tau$ is not vanishing by small, T_1 and T_2 should be field dependent.

Experimental Results on $CHCl_3$

The field dependence of T_1 in $CHCl_3$ for the temperature range from $-30^{\circ}C$ to $+30^{\circ}C$ is shown in FIG. 7 through FIG. 13. The plots show the actual raw data, indicating the scatter was in some cases greater than 10% of the average value. To a great extent, this was due to a low signal-to-noise value for the $CHCl_3$ sample used ($Vs/Vn \sim 20$), the $CHCl_3$ signal being only 1/10th that of an equivalent volume of water. Scatter is also attributed to the graphical method of analysis to be discussed later.

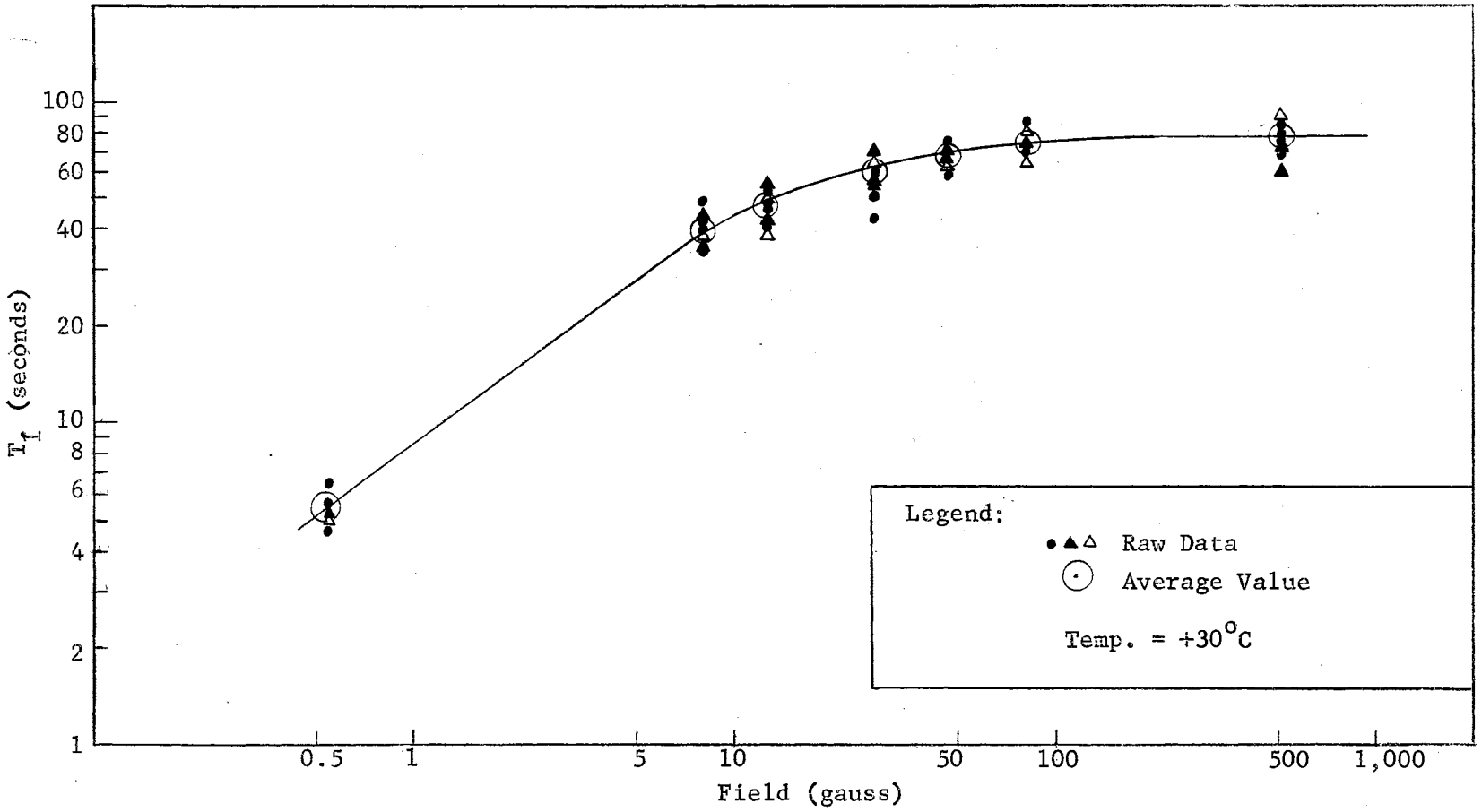

Figure 7. T_1 vs Field For $CHCl_3$, T = 30°C

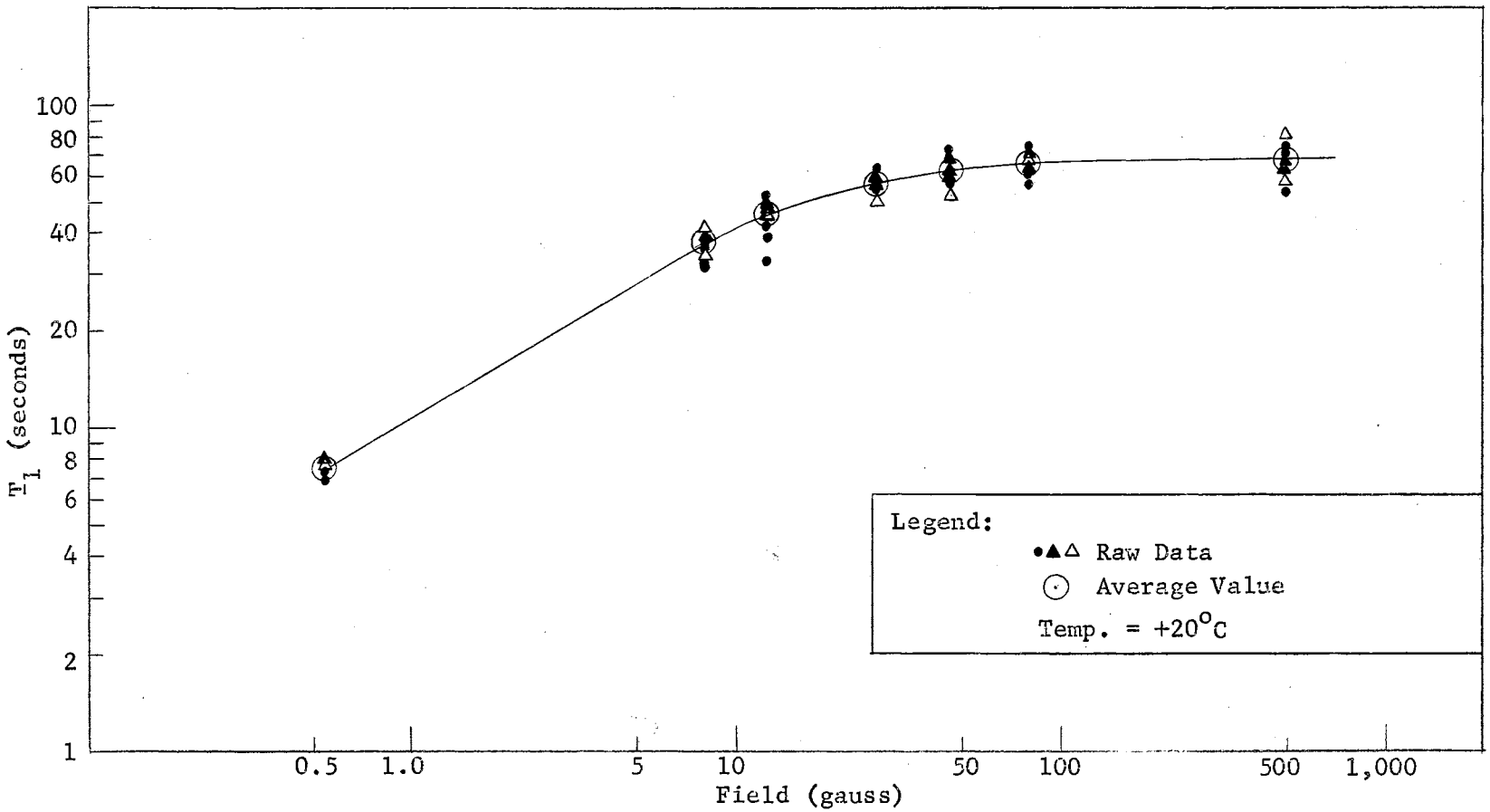

Figure 8. T_1 vs Field For $CHCl_3$, T = 20°C

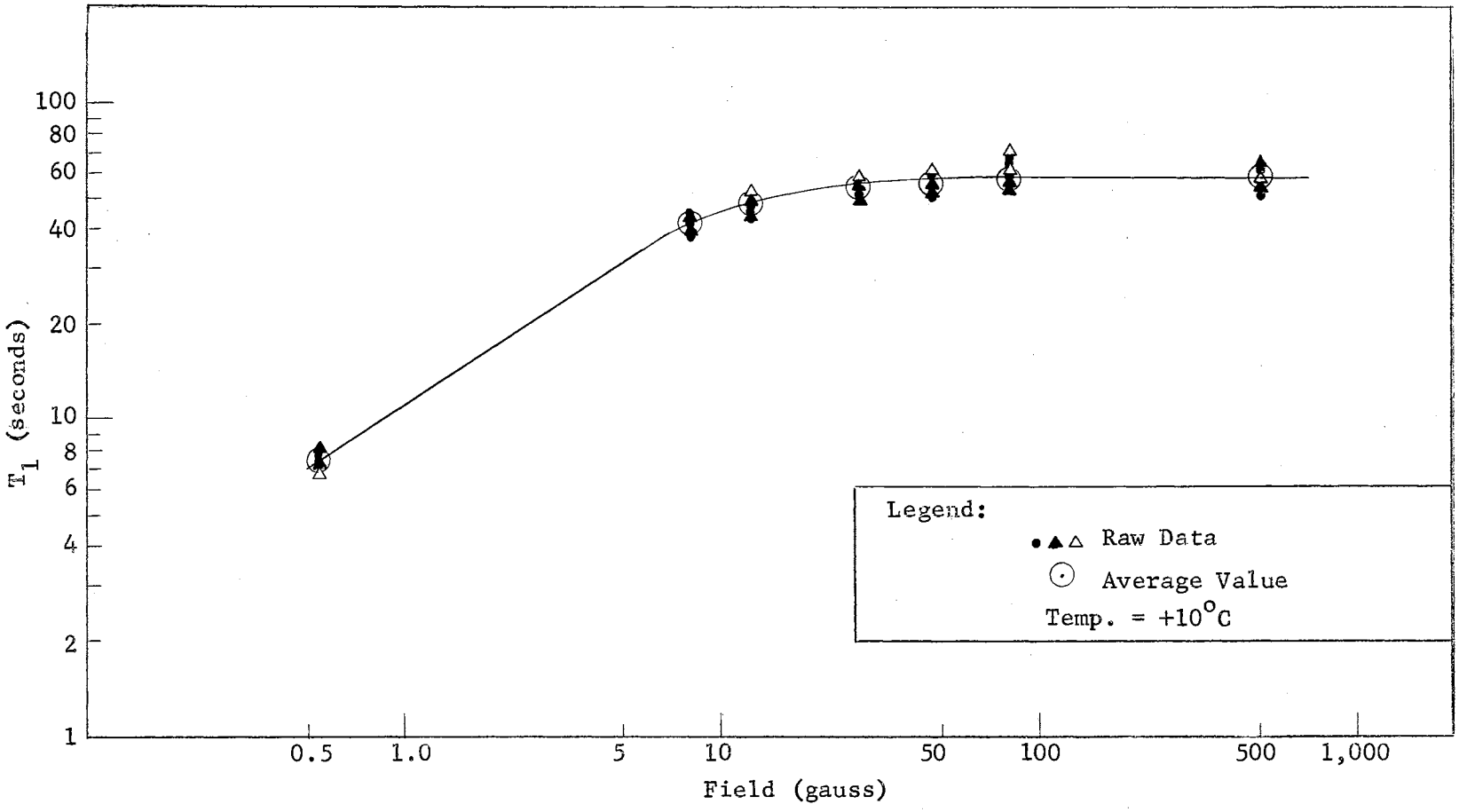

Figure 9. T_1 vs Field For $CHCl_3$, T = 10°C

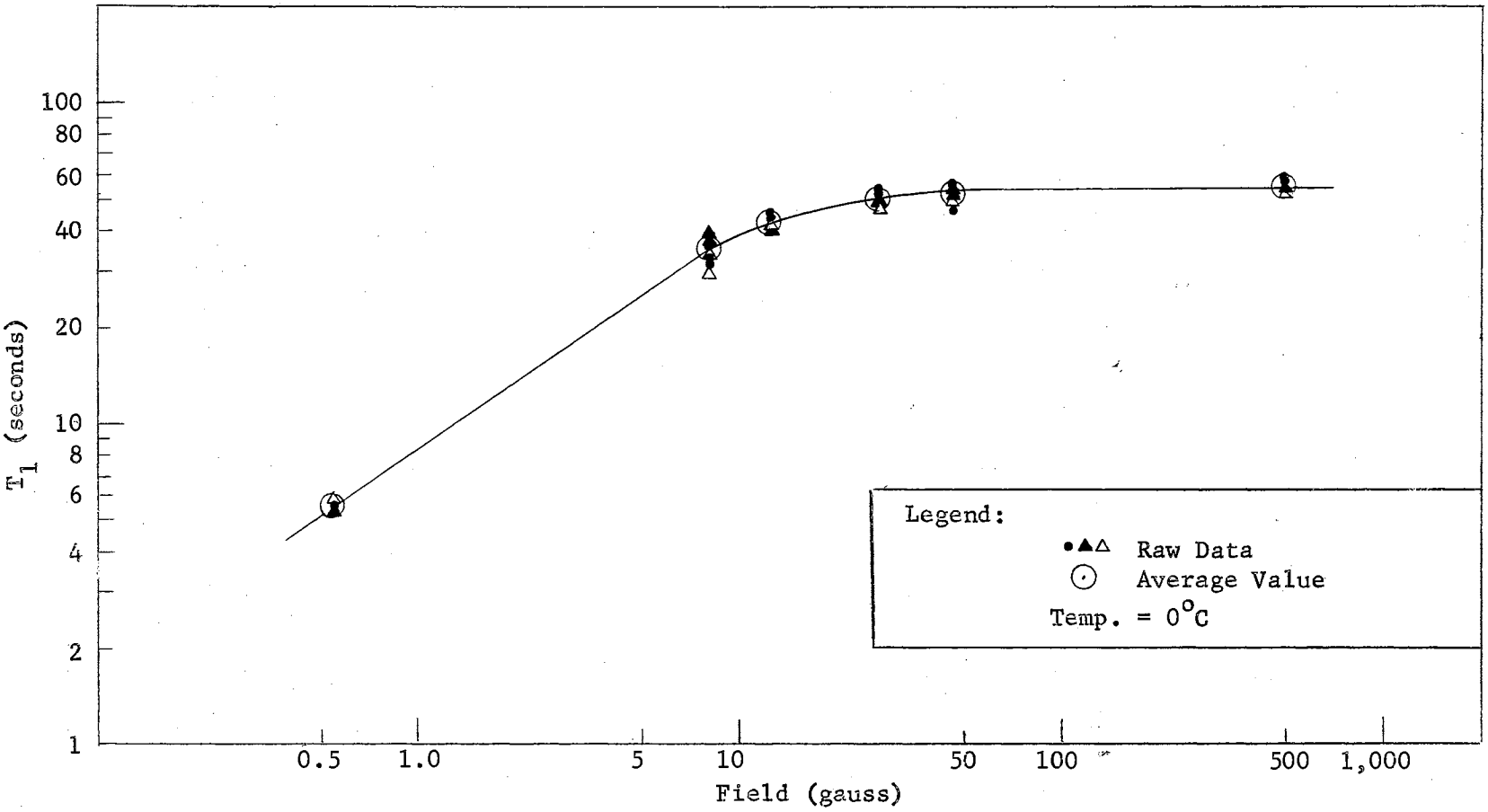

Figure 10. T_1 vs Field For $CHCl_3$, T = 0°C

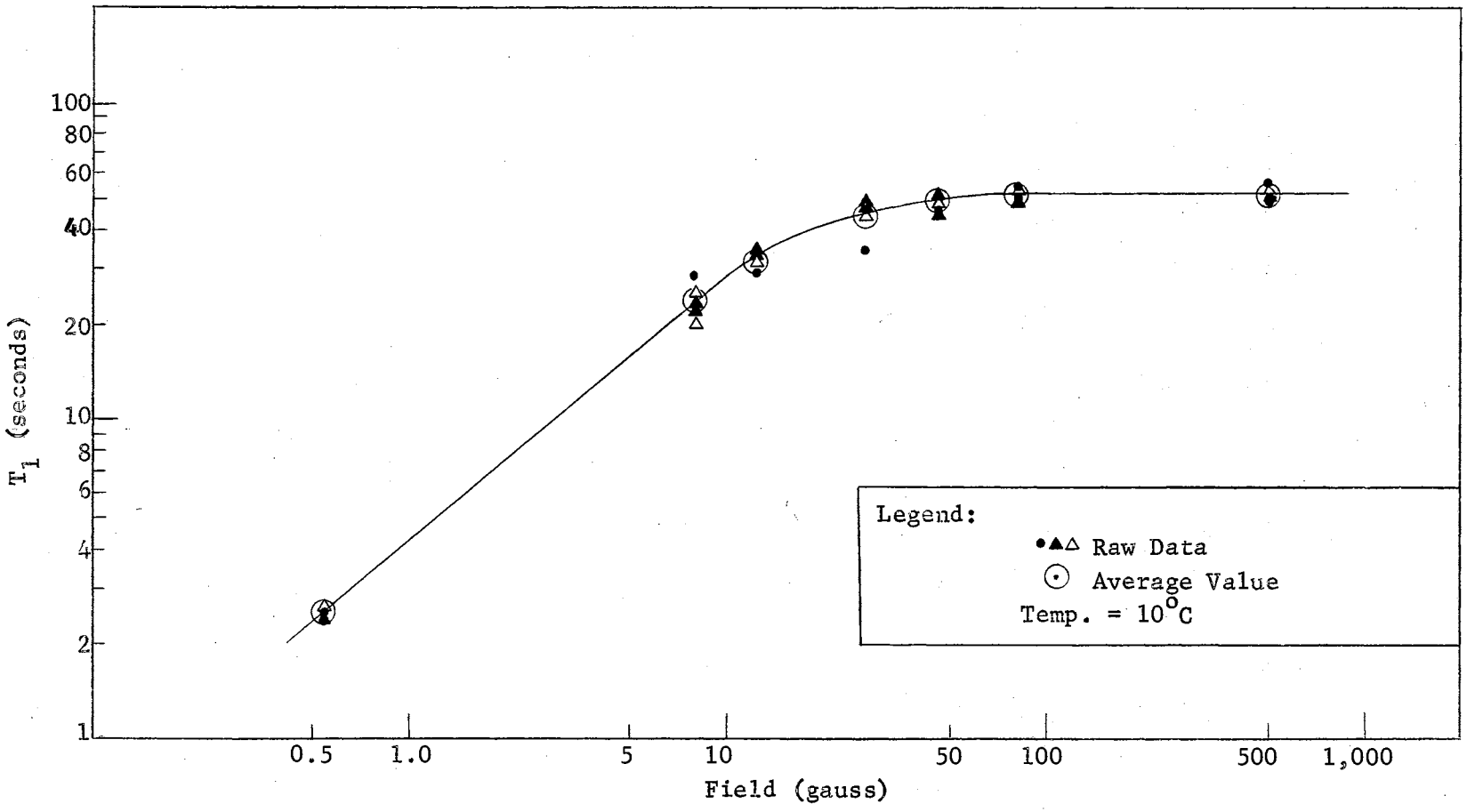

Figure 11. T_1 vs Field For $CHCl_3$, T = -10°C

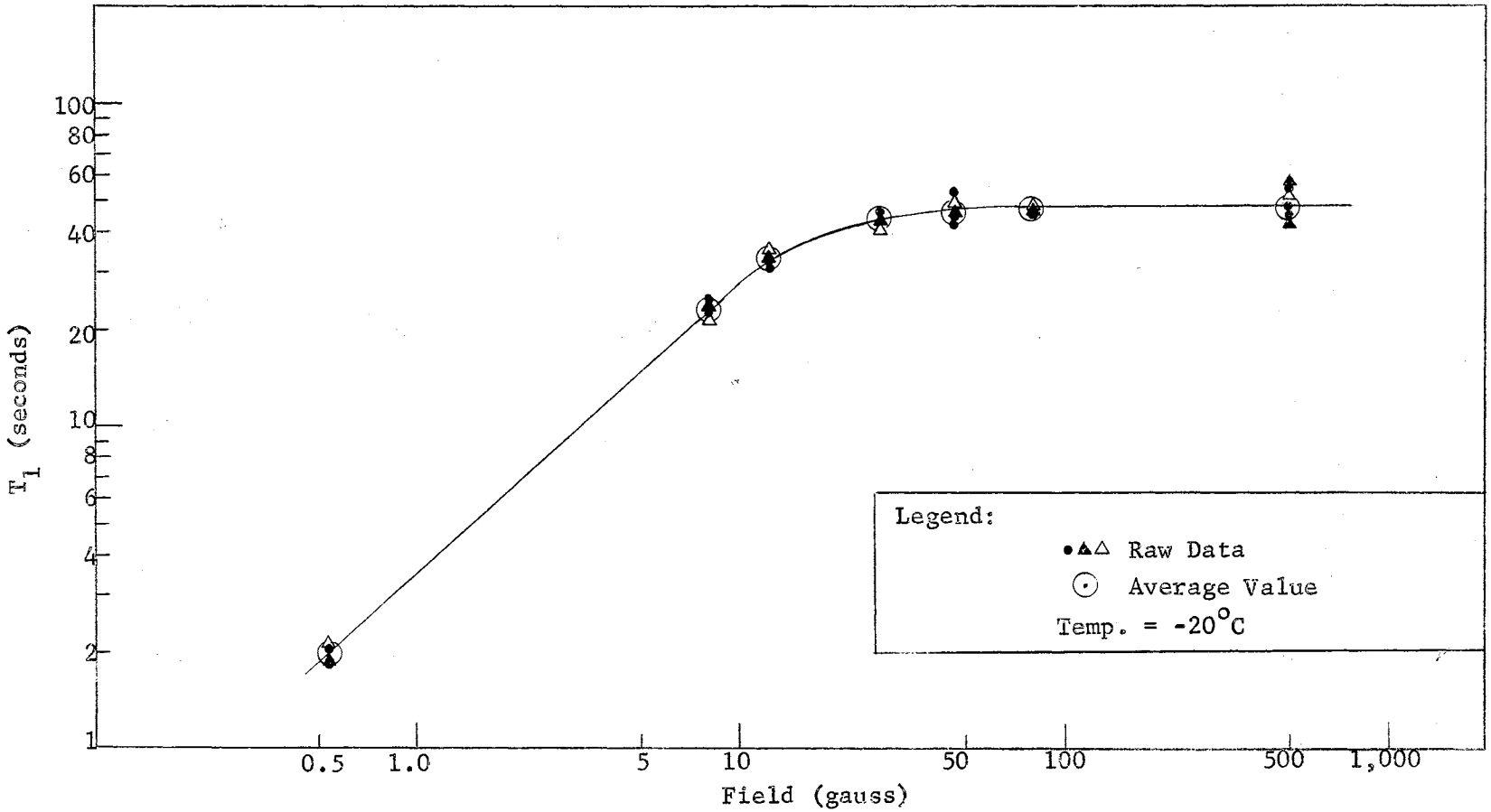

Figure 12. T_1 vs Field For $CHCl_3$, T = -20°C

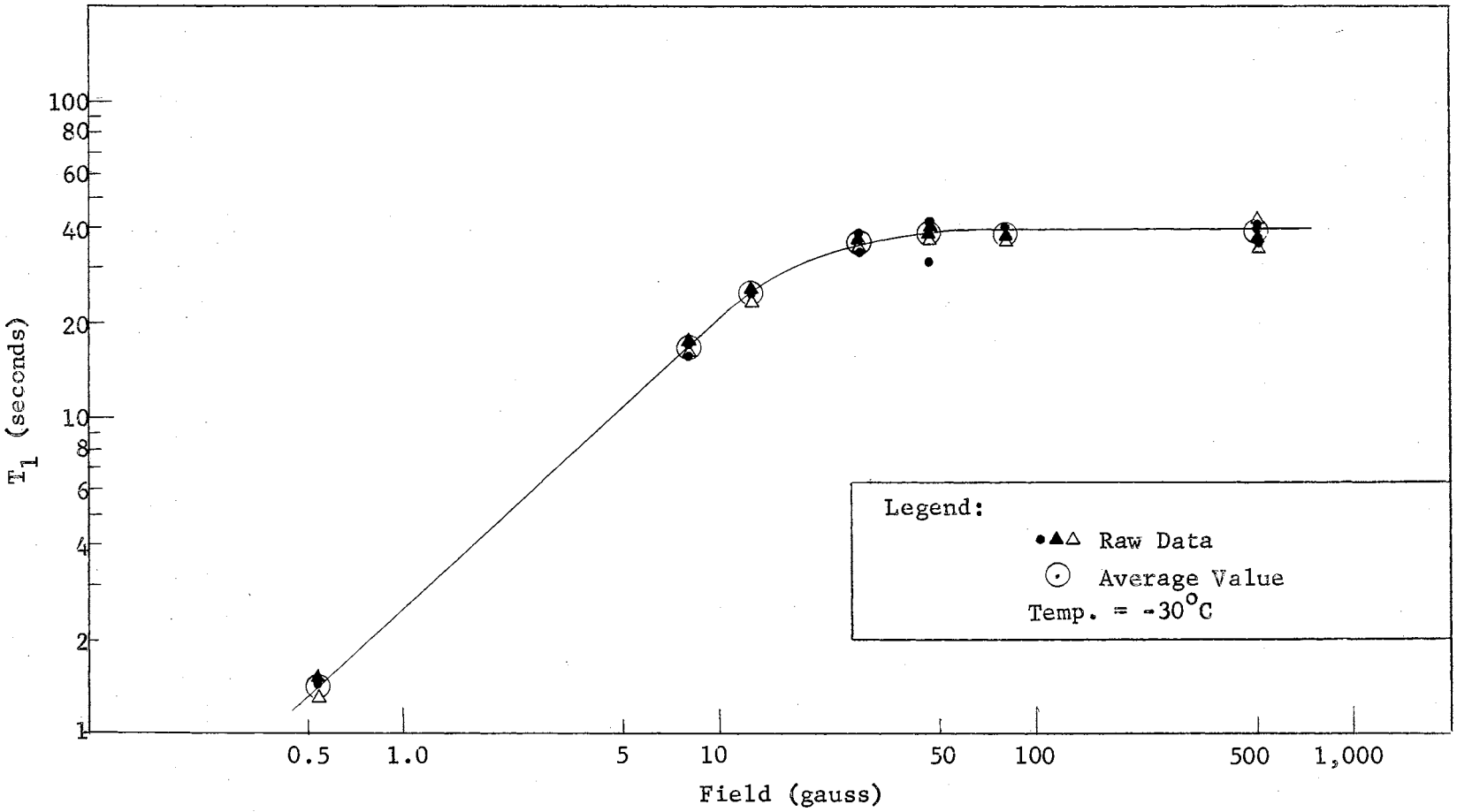

Figure 13. T_1 vs Field For $CHCl_3$, T = -30°C

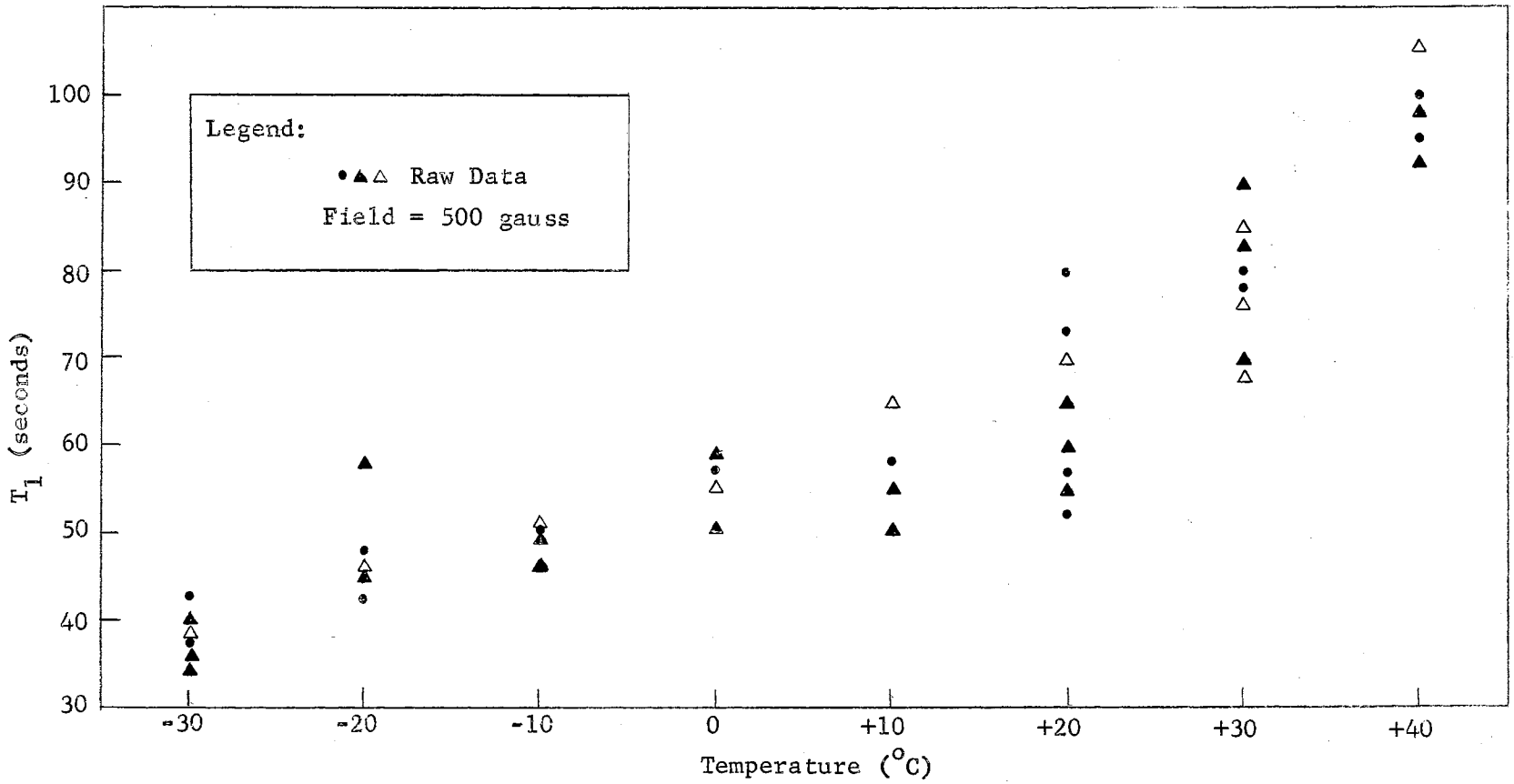

Figure 14. $(T_1)^{obs.}_{500g}$ vs Temperature For $CHCl_3$

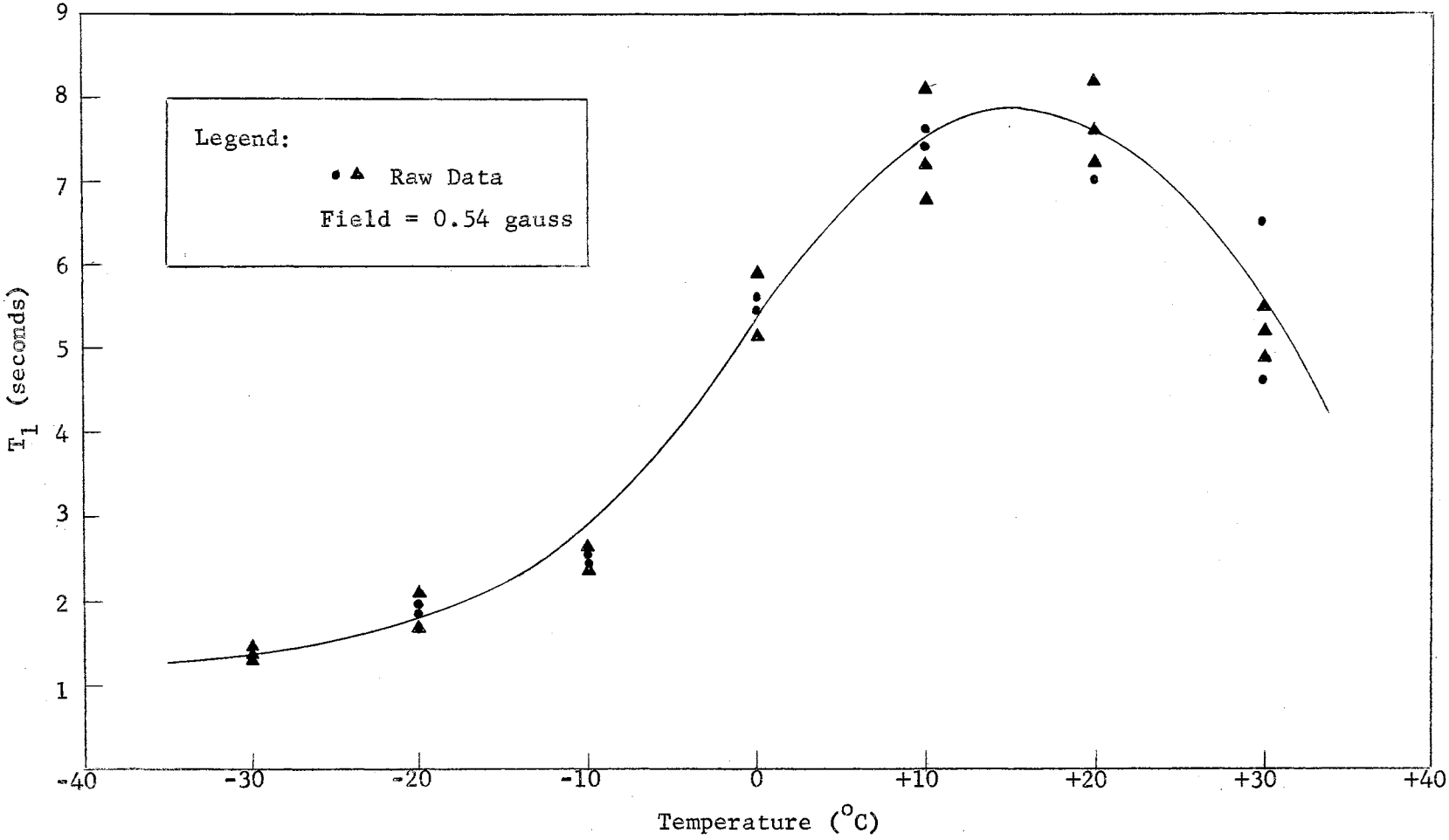

Figure 15. $(T_1)^{obs.}_{0.54g}$ vs Temperature For $CHCl_3$

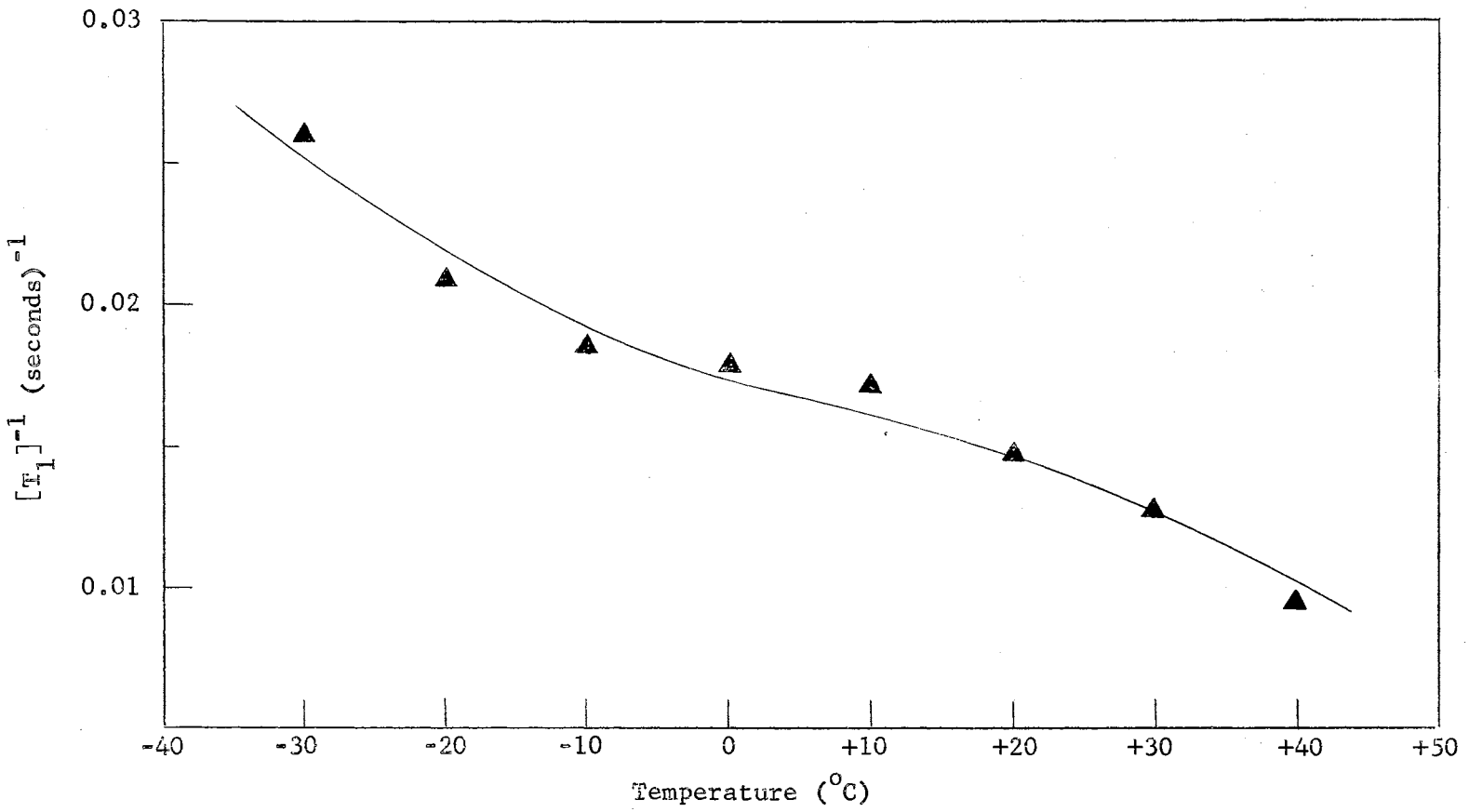

Figure 16. $[T_1]^{-1}$ vs Temperature For $CHCl_3$ at 500 gauss

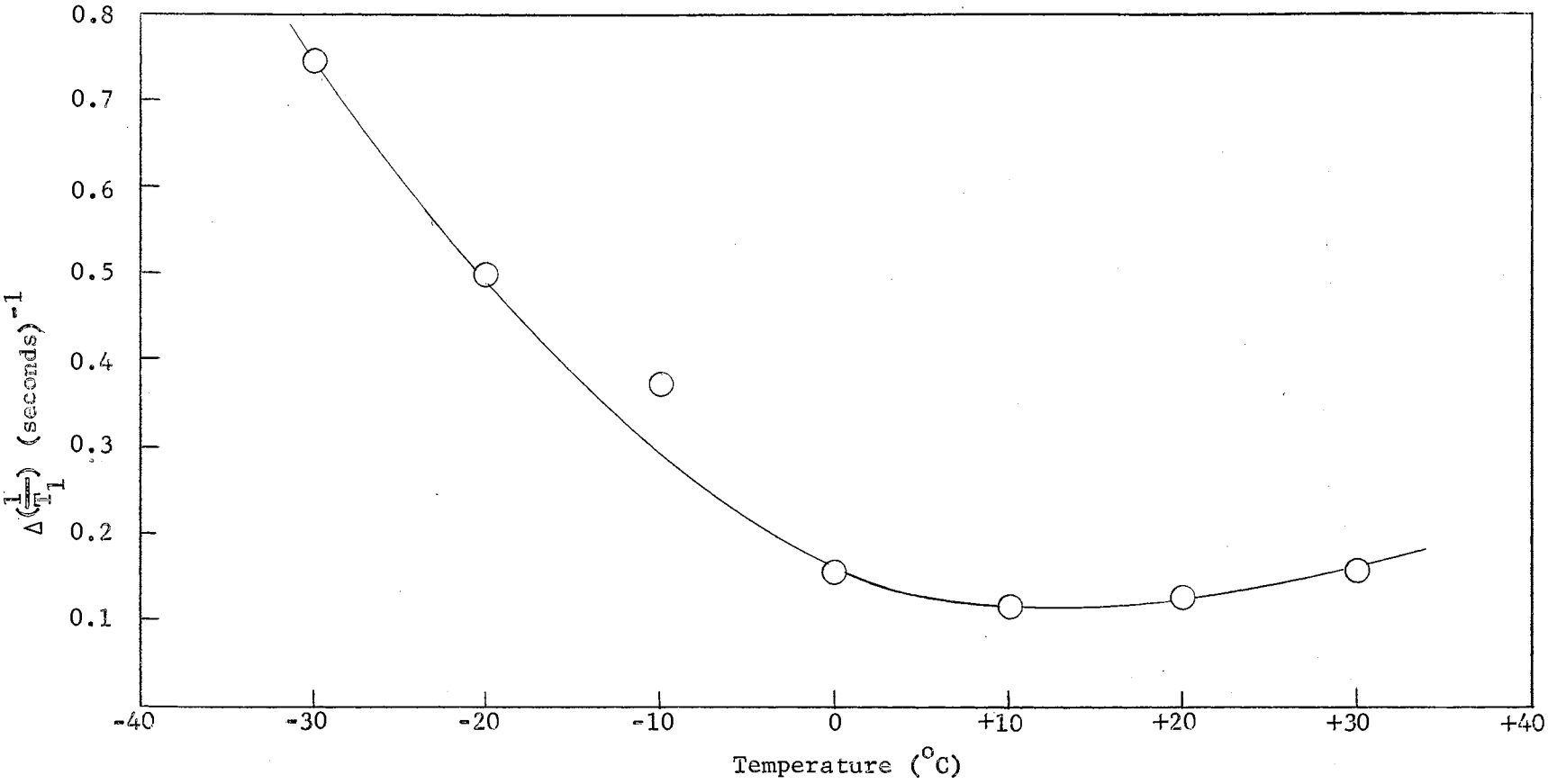

Figure 17. $[T_1]^{-1}$ Indirect Coupling vs Temperature For $CHCl_3$

A plot of T_1 in a field of 500 gauss vs. temperature is shown in FIG. 14, indicating the scatter of the raw data. T_1 in the earth's field (0.54g.) vs. temperature is shown in FIG. 15, also indicating the scatter of the raw data. The temperature dependence of $1/T_1$ in a 500 gauss field is plotted in FIG. 16, using the statistical averages of the raw data. The plot shows an S-shaped behavior for $1/T_1$ which is not predicted theoretically; however, this could easily be caused by inherent scatter in the raw data. Further measurements are planned in the future which will serve to substantiate this $1/T_1$ temperature dependence more clearly.

The temperature dependence of the indirect coupling contribution to $1/T_1$ is shown in FIG. 17, where the equation

$$\left[\Delta \frac{1}{T_1}\right]_{\text{ind. coupling}} = \left[\frac{1}{T_1}\right]_{\text{obs.}} - \left[\frac{1}{T_1^{\infty}}\right] \tag{12}$$

was used to calculate the scalar contribution. T_1^{∞} is the value of T_1 at 500 gauss. The plot in FIG. 17 indicates a minimum value for the scalar contribution occurring at approximately $10^{\circ}C$, for which there seems to be no theoretical evidence. Here again, scatter in the raw data may account for this behavior.

The field dependence of $1/T_1$ for $CHCl_3$ for the temperature range $-30^{\circ}C$ to $+30^{\circ}C$ is plotted in FIG. 18 through FIG. 24. The scalar contribution to $1/T_1$ is also shown on the graphs, $\Delta \frac{1}{T_1}$ calculated from eq. (12). On FIG. 18 and FIG. 19 the experimental results of Ottavi (19) are shown, where $T_1^{\infty} = 28s$. Since no mention is made by Ottavi (19) of the temperature, the assumption is made here that T_1 measurements were performed at room temperature or approximately $25^{\circ}C$. Thus, his results are plotted on two graphs, at $20^{\circ}C$ and $30^{\circ}C$. Somewhat better agreement between his data and the present results is seen at $20^{\circ}C$ if we disregard Ottavi's point at 7.5

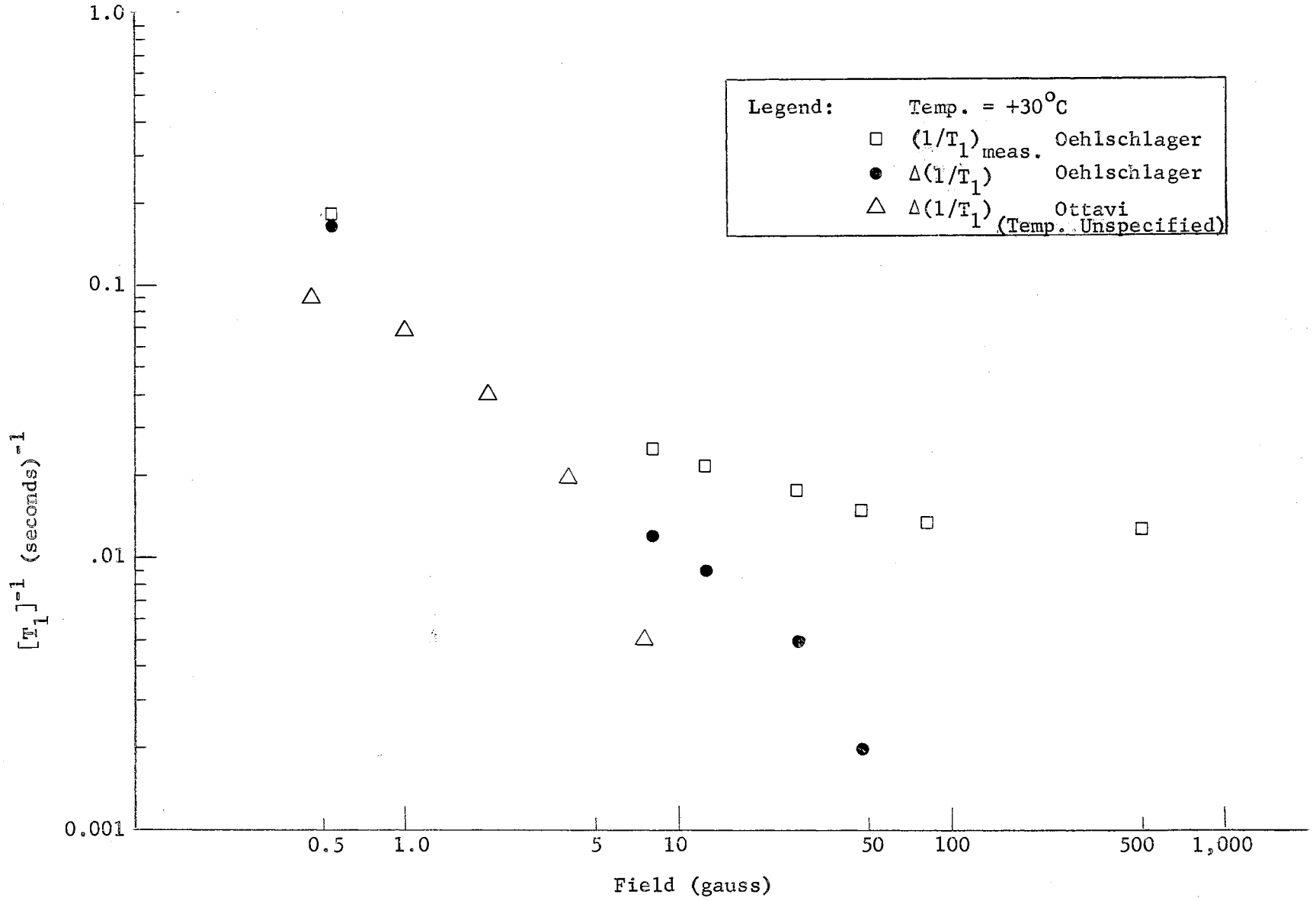

Figure 18. $[T_1]^{-1}$ vs Field For $CHCl_3$, T = +30°C

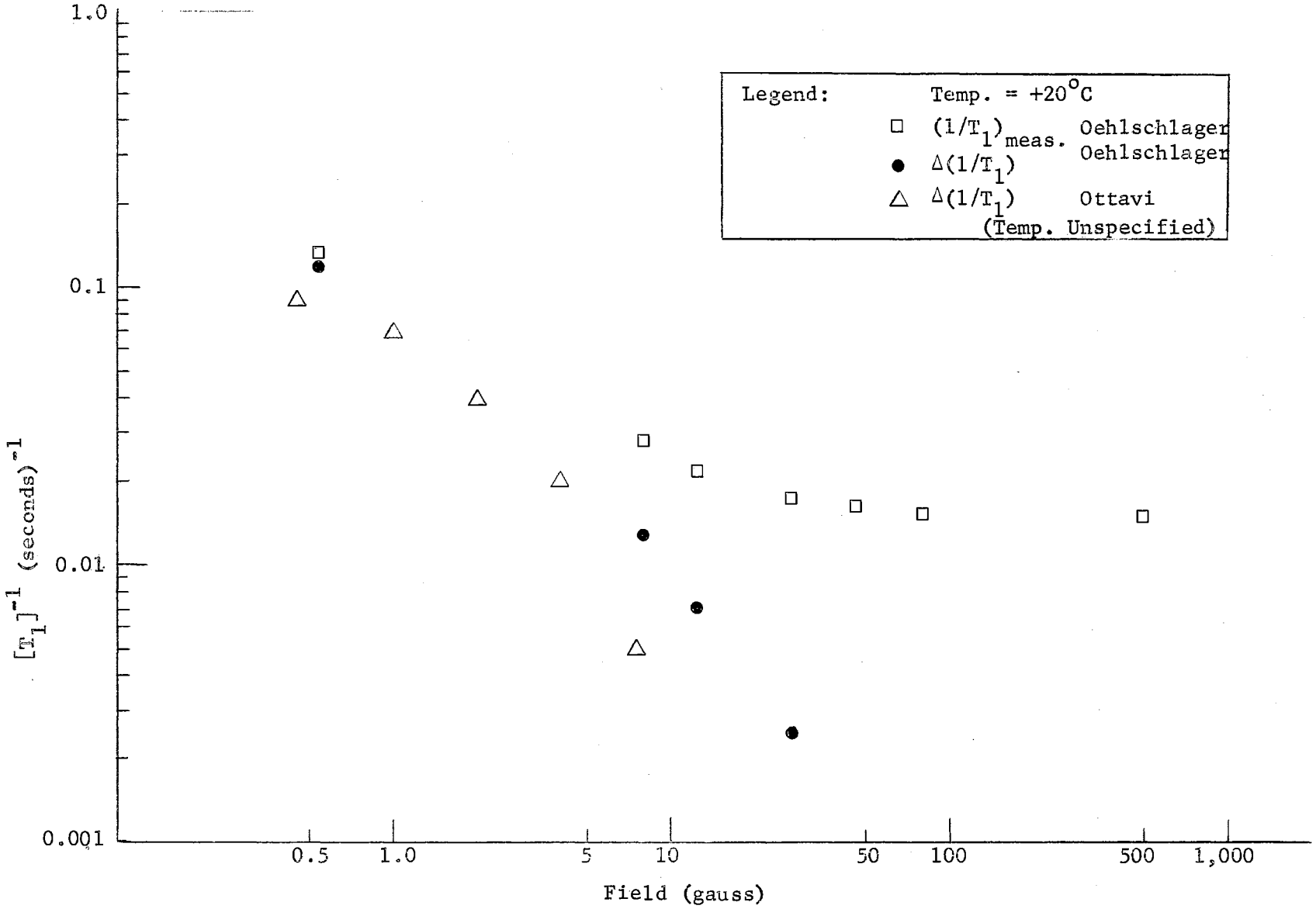

Figure 19. $[T_1]^{-1}$ vs Field For $CHCl_3$, T = +20°C

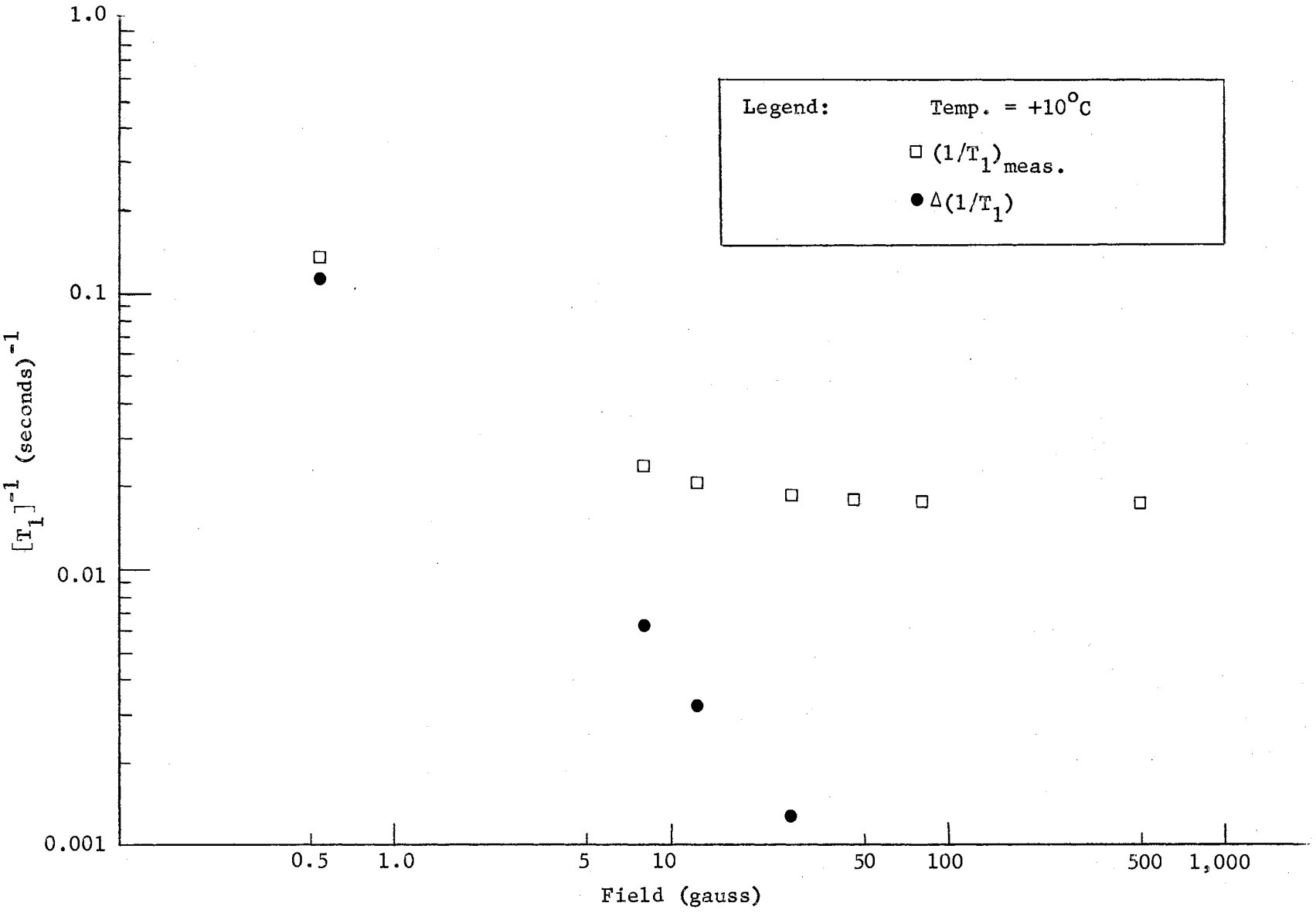

Figure 20. $[T_1]^{-1}$ vs Field For $CHCl_3$, T = +10°C

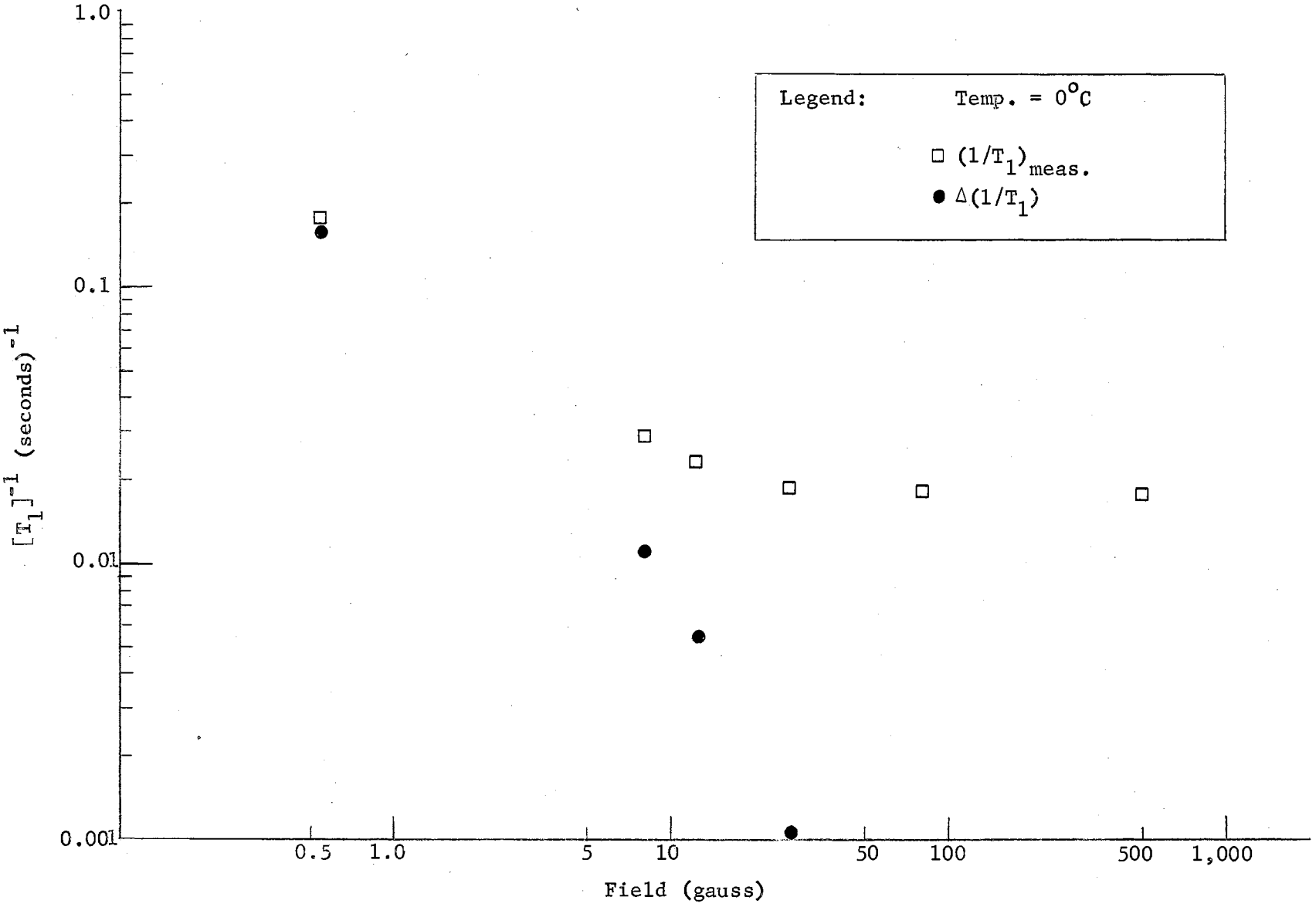

Figure 21. $[T_1]^{-1}$ vs Field For $CHCl_3$, T = 0°C

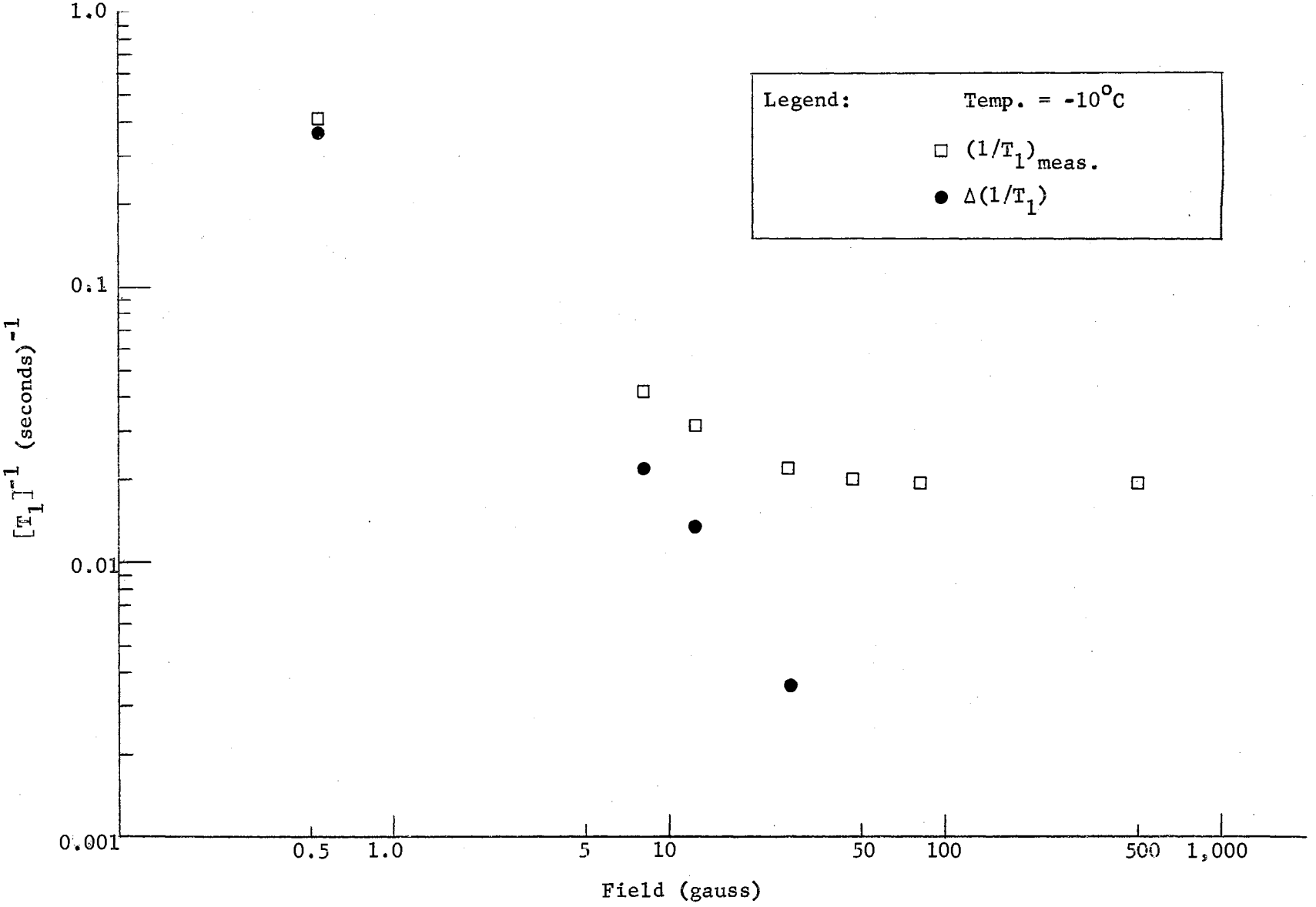

Figure 22. $[T_1]^{-1}$ vs Field For $CHCl_3$, T = -10°C

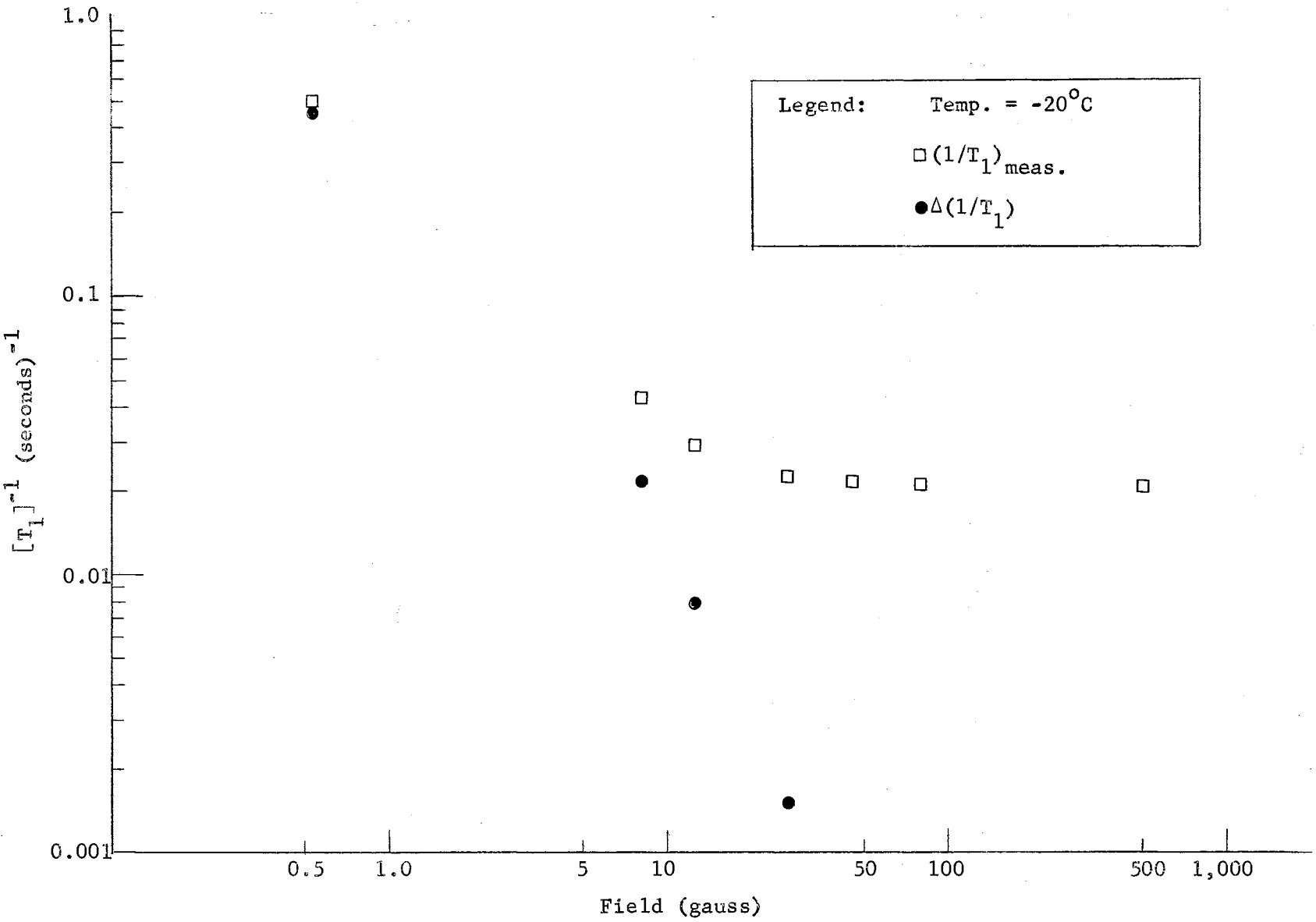

Figure 23. $[T_1]^{-1}$ vs Field For $CHCl_3$, T = -20°C

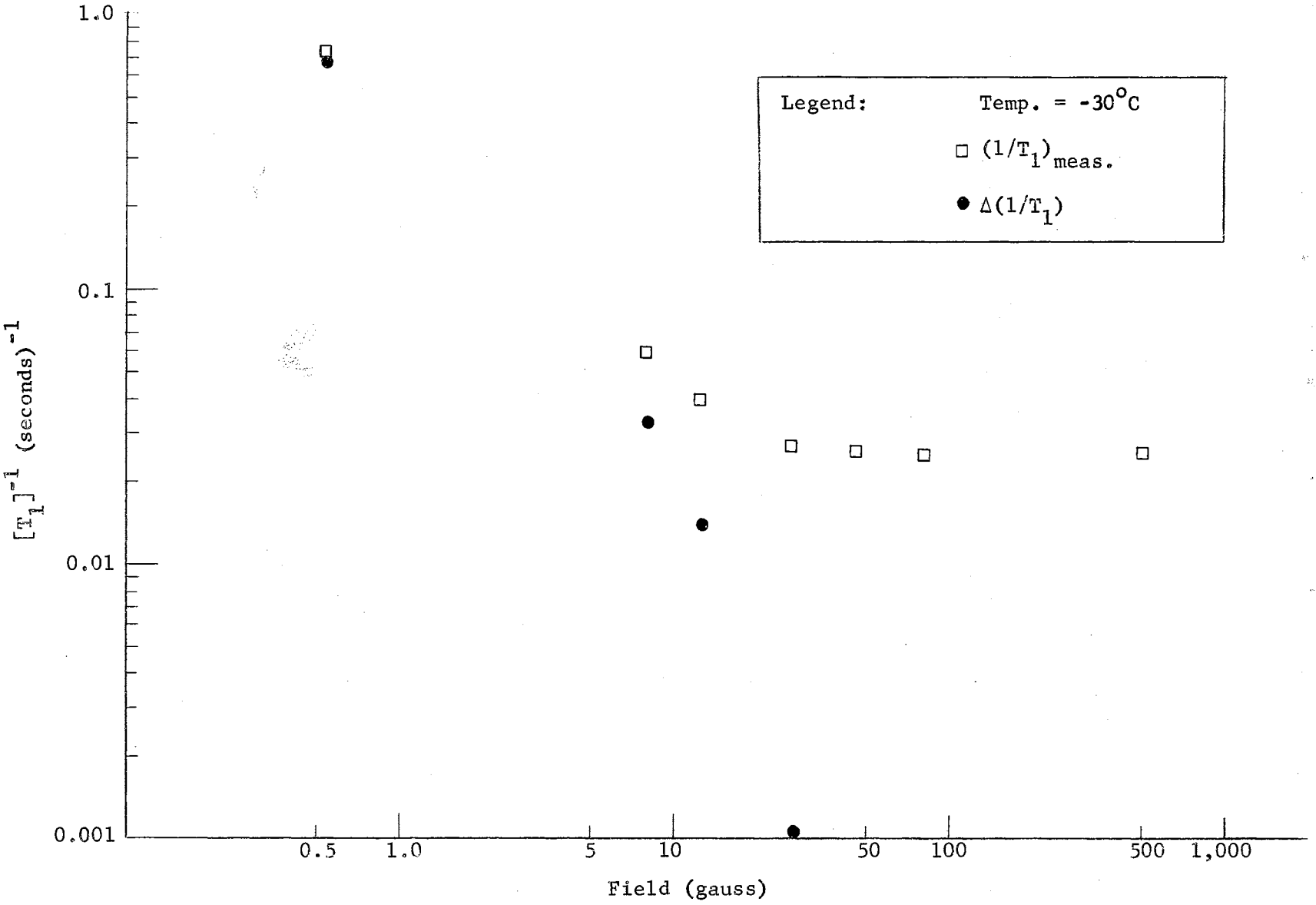

Figure 24. $[T_1]^{-1}$ vs Field For $CHCl_3$, T = -30°C

gauss which is the least reliable since the value of T_1 is very near T_1^{∞} at this field.

The high field value of T_1 obtained by Ottavi was 28 sec, and Winter (20) obtained a value of T_1^{∞} = 42 sec. at 25°C. No mention was made of the de-oxygenation technique employed in either case. Thus, the value obtained here of T_1^{∞} = 78s at 30°C shows the experimental superiority of the de-oxygenation scheme outlined in Chapter I.

A log-log plot of $1/T_1$ in a field of 500 gauss versus $\eta/T(^{\circ}K)$ is shown in FIG. 25, where the temperature dependence of the viscosity, η, was extrapolated to lower temperatures (-30°C). From eq. (9), the expected shape of the log-log plot is linear, however FIG. 25 indicates an S-shaped behavior. This may also be caused by the unusually large scatter in the raw data.

Data Reduction

Three methods were used in determining the longitudinal relaxation time T_1. The two graphical methods used are described in detail by Mitchell (13) and the third method uses a least-squares-fit computer program designed for use on an IBM-1620 computer.

The results of each set of raw data, analyzed by the three techniques, are shown on FIG. 7 through FIG. 15. For a given set of raw data, the three methods of analysis often gave different values of T_1. These different values of T_1 are represented by a common symbol.

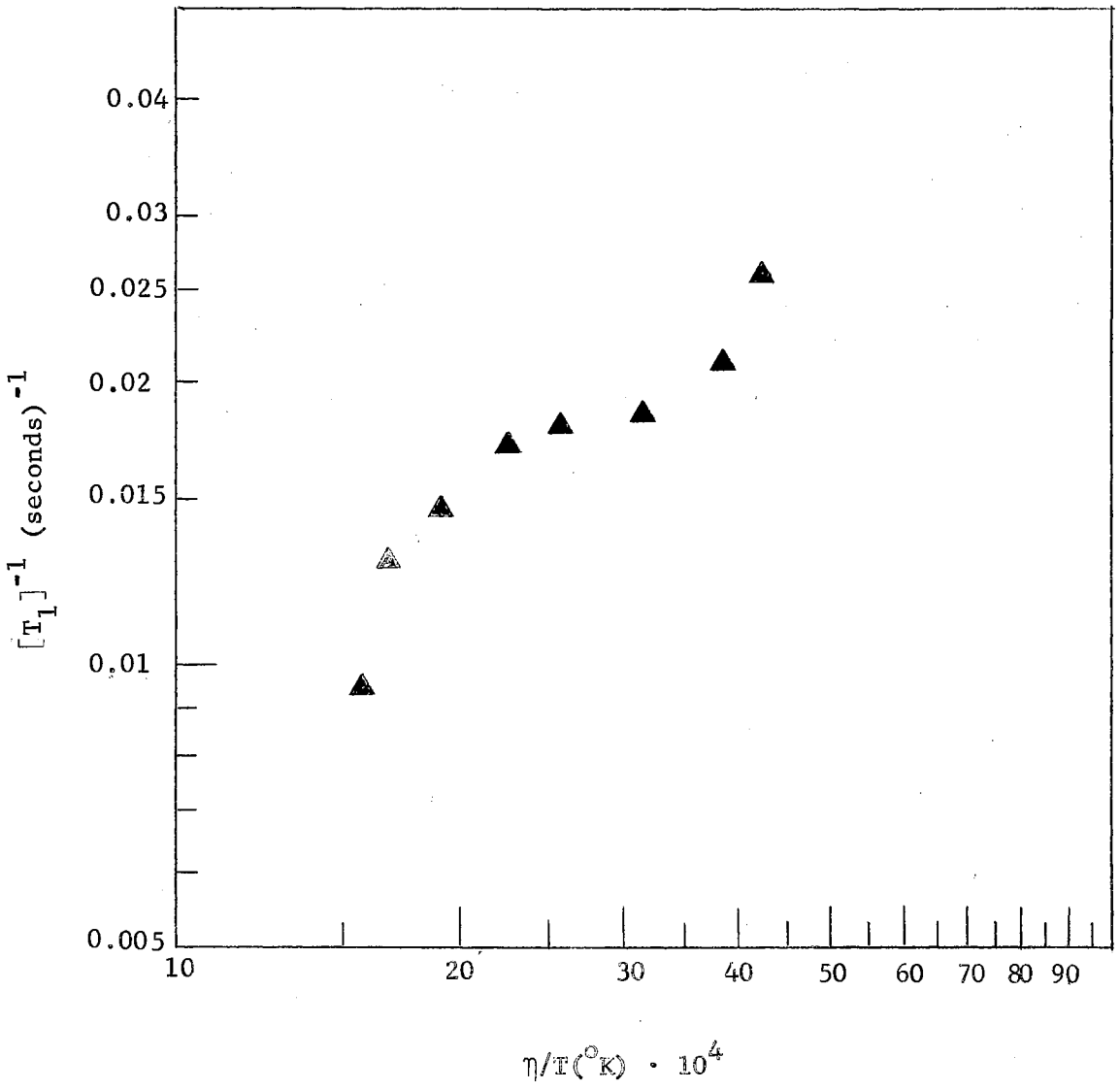

Figure 25. $[T_1]^{-1}_{500g}$ vs $\eta/T(^{\circ}K)$ For $CHCl_3$

BIBLIOGRAPHY

1. Mears and Evans, V. R., J. Soc. Chem. Ind., Lond., 52, 349T, (1933).
2. Risch, C. Biochem. Z., 161, 465, (1925).
3. Peers, A. M., Chem. and Ind., p. 969, (1952).
4. Kolthoff, I. M., Laitimen, H. A., Science, 92, 152 (1940).
5. Mayne, J. E. O., Menter, J. W. and Pryor, M. J., J. Chem. Soc. p. 3229, (1950).
6. Mills, T., and Willis, G. M., J. Electrochem. Soc., 100, 452, (1953).
7. Gilroy D., Mayne, J. E. O., J. Appl. Chem. 12, 382, (1962).
8. Potter, E. C., and White, J. F., J. Appl. Chem., 7, 309, 317, (1957).
9. Arthur, P., Analytical Chemistry, 36, 701, (1964).
10. Fieser, L. F., J. Am. Chem. Soc. 46, 2639, (1924).
11. Kolthoff, I. M., Lingane, J. J., "Pollarography," Vol. I, 2nd ed, p. 396, Intersicence, New Yori, (1952).
12. Meiter, L., Meiter, T., Anal. Chem., 20, 984, (1948).
13. Mitchell, Don E., M.S. Thesis, OSU, (1964).
14. Paules, J. G., and Cutler, D., Nature, 184, 1123 (1959).
15. Nederbragt, Reilly, J. Chem. Phys., 24, 1110, (1956).
16. A. Abragam, The Principles of Nuclear Magnetism (Oxford Univ. Press, London, 1961) pp. 313-315, 298-300, 331.
17. Y. Masuda, J. Phys. Soc. Japan, 11, 670, (1956).
18. Molecular Structure, Wheatley, Oxford, p. 47, (1959).
19. Ottavi, H., Comptes Rendes, 252, 1439, (1961).
20. Winter, J. R., Comptes Rendes, 249, 1346, (1959).

VITA

Walter Keith Oehlschlager

Candidate for the Degree of

Master of Science

Thesis: DESIGN AND DEVELOPMENT OF DE-OXYGENATION SYSTEM AND TEMPERATURE CONTROL APPARATUS FOR NUCLEAR SPIN RELAXATION EXPERIMENTS

Major Field: Physics

Biographical:

Personal Data: Born in Hartford, Connecticut, October 16, 1942, the son of Allen and Kay Oehlschlager.

Education: Attended grade school and high school in Yale, Oklahoma; received a Bachelor of Science degree from Oklahoma State University, Stillwater, Oklahoma, in May, 1962; completed requirements for the Master of Science degree in January, 1965.

Organizations: Member of Sigma Pi Sigma, Phi Eta Sigma, Omicron Delta Kappa and Phi Kappa Phi.